Thermoelastic behavior of advanced composite sandwich plates by using a new 6 unknown quasi-3D hybrid type HSDT

JL Mantari[+1], EV Granados[ϕ]

[+]Faculty of Mechanical Engineering, University of Engineering and Technology, Av. Cascanueces 2281, Santa Anita, Lima, Perú

[ϕ]Faculty of Mechanical Engineering, National University of Engineering, Av. Túpac Amaru 210, Rimac, Lima, Perú.

Abstract. This paper presents an analytical solution for the thermoelastic bending analysis of advanced composite sandwich plates by using a new quasi-3D hybrid type HSDT with 6 unknowns which is based on a generalized formulation. In addition, the nonlinear term of the temperature field is included in the generalized mathematical formulation in such way that it can be freely chosen and if desired can be different from the shear strain shape functions of the displacement field. So, infinite quasi-3D hybrid type HSDTs with just 6 unknowns can be derived from the present generalized formulation. The thermoelastic bending governing equations are obtained through the principle of virtual works and solved via Navier Method. Interesting results are obtained and compared with quasi-3D and 2D HSDTs. Transverse shear stress results are strongly influenced by nonlinear temperature field and for different HSDTs different results are produced. Therefore should be further discussed in the literature.

---

[1]Corresponding Author email: jmantari@utec.edu.pe Tel: +00511 3540070; Cell: +0051 96224551;

Keywords: Shear deformation; Thermoelastic bending analysis; Thermal load; Functionally graded material; Sandwich plate.

1. Introduction

Functionally graded materials (FGMs) are a type of heterogeneous composite material in which the properties change gradually over one or more directions. This material is produced by mixing two or more materials in a certain volume ratio (commonly ceramic and metal). FGMs have been proposed [1], developed and successfully used in industrial applications since 1980's [2]. Its counterpart, classical composites structures such as fiber reinforced plastics (FRPs) suffer from discontinuity of material properties at the interface of the layers and constituents. The continuous nature of the variation of the material properties in FGMs lessens the stress concentrations which become troublesome in a classical composites structure. FGMs were initially designed as a thermal barrier for aerospace structures and fusion reactors. They are now being developed for general use as structural components subjected to high temperatures. Nowadays, FGMs are an alternative materials widely used in aerospace, nuclear, civil, automotive, optical, biomechanical, electronic, chemical, mechanical and shipbuilding industries.

On other hand, many shear deformation theories have been developed over the last years for the analysis of structural elements. These theories can be divided in two groups by a simple criterion: shear deformation theories with thickness stretching effect and shear deformation theories without thickness stretching effect. When a theory includes the thickness stretching effect, the transverse displacement is considered dependent by thickness coordinates obeying the Koiter's recommendation [3], i.e., $\varepsilon_{zz} \neq 0$. In the literature many theories that include thickness stretching effect to study the static, dynamic and stability behavior of functionally graded (FG) single-layer and sandwich plates subjected to thermal or/and mechanical load can be found. Below are listed the most relevant works:

Zenkour [4] investigated the static problem of exponentially graded (EG) rectangular plates subjected to transverse mechanical load using both quasi-3D trigonometric plate theory (TPT) and 3D elasticity solution. The quasi-3D TPT presented in this paper includes the thickness stretching effect, $\varepsilon_{zz} \neq 0$. The thermoelastic bending problem of FG sandwich plates (consisting of a homogeneous core with two FG face-sheet layers) were studied by Zenkour and Alghamdi [5], using a HSDT with thickness stretching effect. The authors modeled nonlinear temperature distribution with a sine function.

Matsunaga [6] modeled the displacement field with power series of the thickness coordinate for the analysis of functionally graded plates (FGPs) under thermal and mechanical loads based on 2D HSDT. Carrera et al. [7] studied the effects of thickness stretching in FGPs and shells under mechanical loads. For analysis, the authors propose several shear deformation theories by using the Carrera's Unified Formulation (CUF). The importance of the transverse normal strain effects in mechanical prediction of stresses for FGPs was pointed out. Neves et al. [8,9] presented a quasi-3D sinusoidal and hyperbolic shear deformation theory ($\varepsilon_{zz} \neq 0$), respectively, for the static and free vibration analysis of FGPs by using collocation with radial basis functions. Mantari and Guedes Soares [10,11,12] developed new quasi-3D HSDTs ($\varepsilon_{zz} \neq 0$) for the study of the static analysis of FGPs. In [10] and [12] the authors presented generalized formulations for the displacement field with two shape functions that are independent of each other. Houari et al. [13] analyzed the sandwich plates with FG skins under thermal load by using a trigonometric HSDT with thickness stretching effect. Readers can also consult the non-polynomial HSDTs presented in Refs. [14-17]. For example, in Sandi et al. [13], in addition to the thermoelasticty analysis of FGMs, as in this paper, they also studied the thermomechanical effect on FGPs.

Many authors use non-polynomial shear strain shape functions, such as trigonometric, trigonometric hyperbolic, exponential, etc. However, the thickness expansion modeling is conditioned by the in-plane displacement model (the transverse non-linear function in the modeling of the thickness expansion is an even function which usually is the derivative of the in-plane non-linear shear strain shape function, i.e. $g(z) = f'(z)$). Therefore, it is not free to choose a different shear strain shape function of the thickness expansion. The present formulation has that freedom, and infinite quasi-3D hybrid type shear deformation theories (polynomial or non-polynomial or hybrid type) can be created just having six unknowns.

In the present paper, a generalized formulation for the thermoelastic bending analysis of FG sandwich plates is presented. This generalized quasi-3D hybrid type HSDT accounts for adequate distribution of the transverse shear stresses through the plate thickness and tangential stress-free boundary conditions on the plate boundary surface, thus

a shear correction factor is not required. The nonlinear term of the temperature field can be different from the shape functions of the displacement field, i.e. is also formulated in generalized manner. The mechanical properties of functionally graded layers of the plate are assumed to vary in the thickness direction according to a power law distribution in terms of the volume fractions of the constituents. The governing equations for the thermoelastic static analysis are obtained through the principle of virtual work. Navier-type analytical solutions are obtained for FG sandwich plates subjected to transverse thermal bi-sinusoidal load for simply supported boundary conditions. The performance of this theory is verified by comparing it with other quasi-3D and 2D HSDTs available in literature. Transverse shear stress results are strongly influenced by nonlinear temperature field and for different HSDTs different results are produced. Therefore should be further discussed in the literature.

2. Theoretical Formulation

The sandwich plates of uniform thickness “h”, length “a”, and width “b” is shown in Figure 1. The rectangular Cartesian coordinate system x, y, z, has the plane z = 0, coinciding with the mid-surface of the plate. The vertical positions of bottom, the two interfaces and the top surface of the sandwich plate are denoted by $h_1 = -h/2$, h_2, h_3, $h_4 = h/2$, respectively. The ratio of the thickness of each layers from bottom to top is denoted by the combination of three numbers, for example, a symmetric sandwich plate composed of three layers of equal thickness will have a configuration or scheme "1-1-1" ($h_2 = -h/6$, $h_3 = h/6$).

2.1. Functionally graded sandwich plates

The material properties for the functionally graded layers vary through the thickness with a power law distribution, which is given below:

$$P^{(k)}{}_{(z)} = (P^{(k)}{}_{t} - P^{(k)}{}_{b})V^{(k)}{}_{(z)} + P^{(k)}{}_{b} \qquad (1)$$

where $P^{(k)}$ denotes the effective material property, $P^{(k)}{}_{t}$ and $P^{(k)}{}_{b}$ denote the property of the top and bottom faces of the functionally graded layer, respectively, and “k” represent a

single-layer of the sandwich plate, i.e., k = 1, 2, 3 for the bottom, middle and top layer, respectively. The effective material properties of the plate, including Young's modulus, E, and shear modulus, G, and the thermal expansion coefficients, "α", vary according to Equation (1). Generally, Poisson's ratio,"ν", varies in a small range. For simplicity, in this paper, "ν" is assumed constant (see Ref. [14]).

The sandwich plate is composed of three layers, an isotropic core and two functionally graded skins as shown in Figure 1. The core is a fully ceramic layer, the bottom layer is made of a mixture of materials from metal to ceramic and the top layer is made of a mixture of materials from ceramic to metal. Therefore, the volume fraction for the ceramic phase $V^{(k)}$ is expressed as (see Figure 2):

$$V^{(1)}{}_{(z)} = \left(\frac{z - h_1}{h_2 - h_1} \right)^p , \; h_1 \le z \le h_2$$

$$V^{(2)}{}_{(z)} = 1, \; h_2 \le z \le h_3$$

$$V^{(3)}{}_{(z)} = \left(\frac{z - h_4}{h_3 - h_4} \right)^p , \; h_3 \le z \le h_4 \qquad \text{(2a-c)}$$

where "p" is the exponent that specifies the material variation profile through the thickness ($0 \le p \le \infty$).

From the above equations can be stated that if the exponent is equal to zero (p=0), the layer acquires the material properties of the top surface. Likewise, if the exponent is equal to infinity (p=∞), the layer acquires the material properties of the bottom surface. These considerations are important when studying a homogeneous material.

2.2. Displacement base field

The generalized displacement field satisfying the conditions of transverse shear stresses (and hence strains) vanishing at a point (x, y, $\pm h/2$) on the outer (top) and inner (bottom) surfaces of the plate, is given as follows (see Mantari and Guedes Soares [10]):

$$\bar{u}(x,y,z) = u(x,y) + z\left[y^{*}\theta_1 + q^{*}\frac{\partial\theta_3}{\partial x} - \frac{\partial w}{\partial x}\right] + f(z)\theta_1,$$

$$\bar{v}(x,y,z) = v(x,y) + z\left[y^{*}\theta_2 + q^{*}\frac{\partial\theta_3}{\partial y} - \frac{\partial w}{\partial y}\right] + f(z)\theta_2, \qquad \text{(3a-c)}$$

$$\bar{w}(x,y,z) = w + g(z)\theta_3,$$

where $u(x,y)$, $v(x,y)$, $w(x,y)$, $\theta_1(x,y)$, $\theta_2(x,y)$ and $\theta_3(x,y)$ are the six unknown displacement functions of middle surface of the plate, whilst $y^{*} = -f'(\frac{h}{2})$ and $q^{*} = -g(\frac{h}{2})$. It is important to mention that $f'(z)$ and $g(z)$ must be even functions. The possibility of having $g(z) \neq f'(z)$ (if desired) allows creating infinite quasi-3D hybrid type HSDTs. In this paper $f(z)$ and $g(z)$ are as follows:

$$f(z) = h\tanh(\frac{z}{h})e^{-\left(\frac{z}{h}\right)^2}\ ;\ g(z) = \cos(\frac{\pi z}{h}) \qquad \text{(4a,b)}$$

Note that such shear strain shape functions can be further optimized to get close to 3D solutions as in [12].

2.3. Kinematic relations and constitutive relations

In the derivation of the necessary equations, small strains are assumed (i.e., displacements and rotations are small, and obey Hooke's law). The linear strain expressions derived from the displacement model of Equations (3a-c), valid for thin, moderately thick and thick plate under consideration are as follows:

$$\varepsilon_{xx} = \varepsilon_{xx}^{0} + z\varepsilon_{xx}^{1} + f(z)\varepsilon_{xx}^{2},$$

$$\varepsilon_{yy} = \varepsilon_{yy}^{0} + z\varepsilon_{yy}^{1} + f(z)\varepsilon_{yy}^{2},$$

$$\varepsilon_{zz} = g'(z)\varepsilon_{zz}^{5},$$

$$\varepsilon_{yz} = \varepsilon_{yz}^{0} + g(z)\varepsilon_{yz}^{3} + f'(z)\varepsilon_{yz}^{4},$$

$$\varepsilon_{xz} = \varepsilon_{xz}^{0} + g(z)\varepsilon_{xz}^{3} + f'(z)\varepsilon_{xz}^{4},$$

$$\varepsilon_{xy} = \varepsilon_{xy}^{0} + z\varepsilon_{xy}^{1} + f(z)\varepsilon_{xy}^{2}. \qquad \text{(5a-f)}$$

where

$$\varepsilon_{xx}^{0} = \frac{\partial u}{\partial x}, \qquad \varepsilon_{xx}^{1} = y^{*}\frac{\partial \theta_1}{\partial x} + q^{*}\frac{\partial^2 \theta_3}{\partial x^2} - \frac{\partial^2 w}{\partial x^2}, \qquad \varepsilon_{xx}^{2} = \frac{\partial \theta_1}{\partial x},$$

$$\varepsilon_{yy}^{0} = \frac{\partial v}{\partial y}, \qquad \varepsilon_{yy}^{1} = y^{*}\frac{\partial \theta_2}{\partial y} + q^{*}\frac{\partial^2 \theta_3}{\partial y^2} - \frac{\partial^2 w}{\partial y^2}, \qquad \varepsilon_{yy}^{2} = \frac{\partial \theta_2}{\partial y},$$

$$\varepsilon_{zz}^{5} = \theta_3,$$

$$\varepsilon_{yz}^{0} = y^{*}\theta_2 + q^{*}\frac{\partial \theta_3}{\partial y}, \qquad \varepsilon_{yz}^{3} = \frac{\partial \theta_3}{\partial y}, \qquad \varepsilon_{yz}^{4} = \theta_2,$$

$$\varepsilon_{xz}^{0} = y^{*}\theta_1 + q^{*}\frac{\partial \theta_3}{\partial x}, \qquad \varepsilon_{xz}^{3} = \frac{\partial \theta_3}{\partial x}, \qquad \varepsilon_{xz}^{4} = \theta_1,$$

$$\varepsilon_{xy}^{0} = \frac{\partial v}{\partial x} + \frac{\partial u}{\partial y}, \qquad \varepsilon_{xy}^{1} = y^{*}\left(\frac{\partial \theta_2}{\partial x} + \frac{\partial \theta_1}{\partial y}\right) + 2q^{*}\left(\frac{\partial^2 \theta_3}{\partial x \partial y}\right) - 2\frac{\partial^2 w}{\partial x \partial y}, \qquad \varepsilon_{xy}^{2} = \frac{\partial \theta_2}{\partial x} + \frac{\partial \theta_1}{\partial y}$$

(6a-p)

For the functionally graded sandwich plates, the stress–strain relationships for plane-stress state including the thermal effects can be expressed as:

$$\begin{Bmatrix} \sigma_{xx} \\ \sigma_{yy} \\ \sigma_{zz} \\ \tau_{yz} \\ \tau_{xz} \\ \tau_{xy} \end{Bmatrix}^{(k)} = \begin{bmatrix} Q_{11} & Q_{12} & Q_{13} & 0 & 0 & 0 \\ Q_{21} & Q_{22} & Q_{23} & 0 & 0 & 0 \\ Q_{31} & Q_{32} & Q_{33} & 0 & 0 & 0 \\ 0 & 0 & 0 & Q_{44} & 0 & 0 \\ 0 & 0 & 0 & 0 & Q_{55} & \\ 0 & 0 & 0 & 0 & 0 & Q_{66} \end{bmatrix}^{(k)} \begin{Bmatrix} \varepsilon_{xx} - \alpha T \\ \varepsilon_{yy} - \alpha T \\ \varepsilon_{zz} - \alpha T \\ \gamma_{yz} \\ \gamma_{xz} \\ \gamma_{xy} \end{Bmatrix}^{(k)} \qquad (7)$$

in which, $\sigma = \{\sigma_{xx}, \sigma_{yy}, \sigma_{zz}, \tau_{yz}, \tau_{xz}, \tau_{xy}\}^{\mathrm{T}}$ and $\varepsilon = \{\varepsilon_{xx}, \varepsilon_{yy}, \varepsilon_{zz}, \varepsilon_{yz}, \varepsilon_{xz}, \varepsilon_{xy}\}^{\mathrm{T}}$ are the stresses and the strain vectors with respect to the plate coordinate system; $\bar{T}$={T, T, T, 0, 0, 0}$^{\mathrm{T}}$ is

the temperature distribution vector. The Q_{ij} expressions in terms of engineering constants are given below:

$$Q_{11(z)} = Q_{22(z)} = Q_{33(z)} = \frac{E(z)}{(1-\nu^2)},$$

$$Q_{12(z)} = Q_{13(z)} = Q_{23(z)} = \frac{E(z)\nu}{(1-\nu^2)},$$

$$Q_{44(z)} = Q_{55(z)} = Q_{66(z)} = \frac{E(z)}{2(1+\nu)}. \qquad \text{(8a-c)}$$

The modulus $E(z), G(z) = \frac{E(z)}{2(1+\nu)}$ and the elastic coefficients $Q_{ij}(z)$ and the thermal expansion coefficients "$\alpha_{(z)}$" vary through the thickness according to Equation (1).

The generalized temperature field which varies through the thickness of the plate can be expressed as follows:

$$T(x,y,z) = T_1(x,y) + \frac{z}{h}T_2(x,y) + \frac{\Psi(z)}{h}T_3(x,y) \qquad (9)$$

where T_1, T_2 and T_3 are thermal load.

Note that in Equation (9), the function of the nonlinear term is expressed in general manner, i.e. it can be different from the shear strain shape functions of the displacement field (Equation (3a-c)) if desired. The temperature distribution vector is given as:

$$\overline{T} = \overline{T_1} + \frac{z}{h}\overline{T_2} + \frac{\Psi(z)}{h}\overline{T_3} \qquad (10)$$

where

$$\overline{T_n} = \begin{bmatrix} T_n \\ T_n \\ T_n \\ 0 \\ 0 \\ 0 \end{bmatrix} \quad \text{(n=1,2,3)} \tag{11}$$

2.4. Principle of virtual work (PVW)

The PVW is utilized for the thermoelastic bending problem of FG sandwich plate. The PVW is expressed as:

$$\delta U + \delta V = 0 \tag{12}$$

where δU is the virtual strain energy, δV is the external virtual works due to external load applied to the plate. These expressions can be written as:

$$\delta U = \int_V \left(\sigma_{xx}\delta\varepsilon_{xx} + \sigma_{yy}\delta\varepsilon_{yy} + \sigma_{zz}\delta\varepsilon_{zz} + \tau_{yz}\delta\gamma_{yz} + \tau_{xz}\delta\gamma_{xz} + \tau_{xy}\delta\gamma_{xy} \right) dV \tag{13}$$

$$\delta V = -\int_\Omega q\delta\overline{w}\, d\Omega \tag{14}$$

This paper only considers thermal loads, so the effect of mechanical load is omitted. Finally, Equation (12) is expressed as:

$$\left[\int_{-h/2}^{h/2} \left\{ \int_\Omega \left[\sigma_{xx}\delta\varepsilon_{xx} + \sigma_{yy}\delta\varepsilon_{yy} + \sigma_{zz}\delta\varepsilon_{zz} + \tau_{yz}\delta\gamma_{yz} + \tau_{xz}\delta\gamma_{xz} + \tau_{xy}\delta\gamma_{xy} \right] dxdy \right\} dz \right] = 0, \tag{15}$$

and, then, it can be further simplified to

$$\begin{aligned} &\int_\Omega (N_1\delta\varepsilon_{xx}^0 + M_1\delta\varepsilon_{xx}^1 + P_1\delta\varepsilon_{xx}^2 + N_2\delta\varepsilon_{yy}^0 + M_2\delta\varepsilon_{yy}^1 + P_2\delta\varepsilon_{yy}^2 \\ &+ R_3\delta\varepsilon_{zz}^5 + N_4\delta\gamma_{yz}^0 + Q_4\delta\gamma_{yz}^3 + K_4\delta\gamma_{yz}^4 + N_5\delta\gamma_{xz}^0 + Q_5\delta\gamma_{xz}^3 + K_5\delta\gamma_{xz}^4 \\ &+ N_6\delta\gamma_{xy}^0 + M_6\delta\gamma_{xy}^1 + P_6\delta\gamma_{xy}^2) dxdy = 0 \end{aligned} \tag{16}$$

where N_i, M_i, P_i, Q_i and K_i are the resultants of the following integrations:

$$\{N_i, M_i, P_i\} = \sum_{k=1}^{3}\left[\int_{h_k}^{h_{k+1}} Q_{ij}^{(k)}\varepsilon_j^{(k)}\{\ 1, z, f(z)\ \}dz\right] - \{N_i^T, M_i^T, P_i^T\},\ \text{(i=1,2)}$$

$$\{N_6, M_6, P_6\} = \sum_{k=1}^{3}\left[\int_{h_k}^{zh_{k+1}} Q_{6j}^{(k)}\varepsilon_j^{(k)}\{\ 1, z, f(z)\ \}dz\right],$$

$$\{N_i\} = \sum_{k=1}^{3}\left[\int_{h_k}^{zh_{k+1}} Q_{ij}^{(k)}\varepsilon_j^{(k)}dz\right],\ \text{(i=4,5)}$$

$$\{Q_i, K_i\} = \sum_{k=1}^{3}\left[\int_{h_k}^{h_{k+1}} Q_{ij}^{(k)}\varepsilon_j^{(k)}\{\ g(z), f'(z)\ \}dz\right],\ \text{(i=4,5)}$$

$$\{R_i\} = \sum_{k=1}^{3}\left[\int_{h_k}^{zh_{k+1}} Q_{ij}^{(k)}\varepsilon_j^{(k)}g'(z)dz\right] - R_i^T,\ \text{(i=3)}$$

$$\{N_i^T, M_i^T, P_i^T\} = \sum_{k=1}^{3}\left[\int_{h_k}^{h_{k+1}} \alpha_{(z)}^{(k)}Q_{ij}^{(k)}\overline{T}\{\ 1, z, f(z)\ \}dz\right],\ \text{(i=1,2)}$$

$$\{R_i^T\} = \sum_{k=1}^{3}\left[\int_{h_k}^{h_{k+1}} \alpha_{(z)}^{(k)}Q_{ij}^{(k)}\overline{T}g'(z)dz\right],\ \text{(i=3)} \qquad \text{(17a-g)}$$

2.5. Plate governing equations

Using the generalized displacement–strain relations (Equations (5a-f) and (6a-p)) and stress–strain relations (Equation (7)), and integrating by parts and applying the fundamental lemma of variational calculus and collecting the coefficients of $\delta u, \delta v, \delta w$, $\delta\theta_1, \delta\theta_2, \delta\theta_3$ in Equation (16), the governing equations are obtained as:

$$\delta u: \qquad \frac{\partial N_1}{\partial x} + \frac{\partial N_6}{\partial y} = 0$$

$$\delta v: \quad \frac{\partial N_2}{\partial y}+\frac{\partial N_6}{\partial x}=0$$

$$\delta w: \quad \frac{\partial^2 M_1}{\partial x^2}+\frac{\partial^2 M_2}{\partial y^2}+2\frac{\partial^2 M_6}{\partial y \partial x}=0$$

$$\delta\theta_1: \quad y^*(\frac{\partial M_1}{\partial x}+\frac{\partial M_6}{\partial y}-N_5)+\frac{\partial P_1}{\partial x}+\frac{\partial P_6}{\partial y}-K_5=0$$

$$\delta\theta_2: \quad y^*(\frac{\partial M_2}{\partial y}+\frac{\partial M_6}{\partial x}-N_4)+\frac{\partial P_2}{\partial y}+\frac{\partial P_6}{\partial x}-K_4=0$$

$$\delta\theta_3: \quad q^*(\frac{\partial N_4}{\partial y}+\frac{\partial N_5}{\partial x}-\frac{\partial^2 M_1}{\partial x^2}-\frac{\partial^2 M_2}{\partial y^2}-2\frac{\partial^2 M_6}{\partial y \partial x})+\frac{\partial Q_4}{\partial y}+\frac{\partial Q_5}{\partial x}-R_3=0$$

(18a-f)

By substituting the stress-strain relations into the definitions of force and moment resultants given in Equation (17a-g) the following constitutive equations are obtained:

$$\mathrm{N_i}=\mathrm{A_{ij}}\varepsilon_j^0+B_{ij}\varepsilon_j^1+C_{ij}\varepsilon_j^2+D_{ij}\varepsilon_j^3+E_{ij}\varepsilon_j^4+F_{ij}\varepsilon_j^5-\mathrm{A_{ij}^*}\overline{T_1}-B_{\mathrm{ij}}^*\overline{T_2}^*-C_{\mathrm{ij}}^*\overline{T_3}^*,\ \text{(i=1,2)}$$

$$\mathrm{N_i}=\mathrm{A_{ij}}\varepsilon_j^0+B_{ij}\varepsilon_j^1+C_{ij}\varepsilon_j^2+D_{ij}\varepsilon_j^3+E_{ij}\varepsilon_j^4+F_{ij}\varepsilon_j^5,\ \text{(i=4,5,6)}$$

$$\mathrm{M_i}=\mathrm{B_{ij}}\varepsilon_j^0+G_{ij}\varepsilon_j^1+H_{ij}\varepsilon_j^2+I_{ij}\varepsilon_j^3+J_{ij}\varepsilon_j^4+K'_{ij}\varepsilon_j^5-\mathrm{B_{ij}^*}\overline{T_1}-G_{\mathrm{ij}}^*\overline{T_2}^*-H_{\mathrm{ij}}^*\overline{T_3}^*,\ \text{(i=1,2)}$$

$$\mathrm{M_i}=\mathrm{B_{ij}}\varepsilon_j^0+G_{ij}\varepsilon_j^1+H_{ij}\varepsilon_j^2+I_{ij}\varepsilon_j^3+J_{ij}\varepsilon_j^4,\ \text{(i=6)}$$

$$\mathrm{P_i}=C_{\mathrm{ij}}\varepsilon_j^0+H_{ij}\varepsilon_j^1+L_{ij}\varepsilon_j^2+M'_{ij}\varepsilon_j^3+N'_{ij}\varepsilon_j^4+O_{ij}\varepsilon_j^5-C_{\mathrm{ij}}^{**}\overline{T_1}-H_{\mathrm{ij}}^{**}\overline{T_2}^*-L_{\mathrm{ij}}^{**}\overline{T_3}^*,\ \ \text{(i=1,2)}$$

$$\mathrm{P_i}=C_{\mathrm{ij}}\varepsilon_j^0+H_{ij}\varepsilon_j^1+L_{ij}\varepsilon_j^2+M'_{ij}\varepsilon_j^3+N'_{ij}\varepsilon_j^4+O_{ij}\varepsilon_j^5,\ \text{(i=6)}$$

$$\mathrm{Q_i}=D_{\mathrm{ij}}\varepsilon_j^0+I_{ij}\varepsilon_j^1+M_{ij}\varepsilon_j^2+P'_{ij}\varepsilon_j^3+Q'_{ij}\varepsilon_j^4+R'_{ij}\varepsilon_j^5,\qquad \text{(i=4,5)}$$

$$\mathrm{K_i}=E_{\mathrm{ij}}\varepsilon_j^0+J_{ij}\varepsilon_j^1+N'_{ij}\varepsilon_j^2+Q'_{ij}\varepsilon_j^3+S_{ij}\varepsilon_j^4+T_{ij}\varepsilon_j^5,\ \text{(i=4,5)}$$

$$\mathrm{R_i}=F_{\mathrm{ij}}\varepsilon_j^0+K'_{ij}\varepsilon_j^1+O_{ij}\varepsilon_j^2+R'_{ij}\varepsilon_j^3+T_{ij}\varepsilon_j^4+U_{ij}\varepsilon_j^5-F_{\mathrm{ij}}^*T_1-K'^*_{\mathrm{ij}}T_2^*-O_{\mathrm{ij}}^*T_3^*,\ \text{(i=3)}$$

(19a-i)

where

$$(A_{ij}, B_{ij}, C_{ij}, D_{ij}, E_{ij}, F_{ij})) = \sum_{k=1}^{3} \int_{h_k}^{h_{k+1}} Q_{ij(z)}^{(k)} (1, z, f(z), g(z), f'(z), g'(z)) dz$$

$$(G_{ij}, H_{ij}, I_{ij}, J_{ij}, K'_{ij}) = \sum_{k=1}^{3} \int_{h_k}^{h_{k+1}} Q_{ij(z)}^{(k)} (z^2, zf(z), zg(z), zf'(z), zg'(z)) dz$$

$$(L_{ij}, M'_{ij}, N'_{ij}, O_{ij}) = \sum_{k=1}^{3} \int_{h_k}^{h_{k+1}} Q_{ij(z)}^{(k)} (f^2(z), f(z)g(z), f(z)f'(z), f(z)g'(z)) dz$$

$$(P'_{ij}, Q'_{ij}, R'_{ij}) = \sum_{k=1}^{3} \int_{h_k}^{h_{k+1}} Q_{ij(z)}^{(k)} (g^2(z), g(z)f'(z), g(z)g'(z)) dz$$

$$(S_{ij}, T_{ij}) = \sum_{k=1}^{3} \int_{h_k}^{h_{k+1}} Q_{ij(z)}^{(k)} (f'^2(z), f'(z)g'(z)) dz$$

$$(U_{ij}) = \sum_{k=1}^{3} \int_{h_k}^{h_{k+1}} Q_{ij(z)}^{(k)} (g'^2(z)) dz$$

$$(A_{ij}^*, B_{ij}^*, C_{ij}^*, F_{ij}^*) = \sum_{k=1}^{3} \int_{h_k}^{h_{k+1}} \alpha_{(z)}^{(k)} Q_{ij(z)}^{(k)} (1, z, \Psi(z), g'(z)) dz$$

$$(G_{ij}^*, H_{ij}^*, K'^*_{ij}) = \sum_{k=1}^{3} \int_{h_k}^{h_{k+1}} \alpha_{(z)}^{(k)} Q_{ij(z)}^{(k)} (z^2, z\Psi(z), zg'(z)) dz$$

$$(O_{ij}^*) = \sum_{k=1}^{3} \int_{h_k}^{h_{k+1}} \alpha_{(z)}^{(k)} Q_{ij(z)}^{(k)} (g'(z)\Psi(z)) dz$$

$$(C_{ij}^{**}, H_{ij}^{**}, L_{ij}^{**}) = \sum_{k=1}^{3} \int_{h_k}^{h_{k+1}} \alpha_{(z)}^{(k)} Q_{ij(z)}^{(k)} (f(z), zf(z), f(z)\Psi(z)) dz$$

$T_n^* = T_n / h$ (n=2,3)

(20a-k)

In what follows, the problem under consideration is solved for the simply supported boundary conditions and they are given at all four edges as follows:

$N_1 = M_1 = P_1 = v = w = \theta_2 = \theta_3$ at x = 0, a,

$N_2 = M_2 = P_2 = u = w = \theta_1 = \theta_3$ at y = 0, b. (21a,b)

3. Solution procedure

Navier's procedure along with governing equations (18a-f) allow to obtain solution of the displacement variables satisfying the above boundary conditions. Such displacement variables (six unknowns) can be expressed in the following Fourier series:

$$u(x,y)=\sum_{r=1}^{\infty}\sum_{s=1}^{\infty}U_{rs}\cos(\lambda x)\sin(\beta y), \qquad 0\le x\le a;\quad 0\le y\le b \tag{22a}$$

$$v(x,y)=\sum_{r=1}^{\infty}\sum_{s=1}^{\infty}V_{rs}\sin(\lambda x)\cos(\beta y), \qquad 0\le x\le a;\quad 0\le y\le b \tag{22b}$$

$$w(x,y)=\sum_{r=1}^{\infty}\sum_{s=1}^{\infty}W_{rs}\sin(\lambda x)\sin(\beta y), \qquad 0\le x\le a;\quad 0\le y\le b \tag{22c}$$

$$\theta_1(x,y)=\sum_{r=1}^{\infty}\sum_{s=1}^{\infty}\Theta^1_{rs}\cos(\lambda x)\sin(\beta y), \qquad 0\le x\le a;\quad 0\le y\le b \tag{22d}$$

$$\theta_2(x,y)=\sum_{r=1}^{\infty}\sum_{s=1}^{\infty}\Theta^2_{rs}\sin(\lambda x)\cos(\beta y), \qquad 0\le x\le a;\quad 0\le y\le b \tag{22e}$$

$$\theta_3(x,y)=\sum_{r=1}^{\infty}\sum_{s=1}^{\infty}\Theta^3_{rs}\sin(\lambda x)\sin(\beta y), \qquad 0\le x\le a;\quad 0\le y\le b \tag{22f}$$

where

$$\lambda=\frac{r\pi}{a},\ \beta=\frac{s\pi}{b} \tag{23}$$

The transverse thermal loads T_1, T_2, T_3 are also expanded in the double-Fourier sine series as:

$$T_i(x,y)=\sum_{r=1}^{\infty}\sum_{s=1}^{\infty}T^i_{mn}\sin(\lambda x)\sin(\beta y)\ ,\ (\text{i=1,2,3}) \tag{24}$$

where

$T^i_{mn}=\hat{T}_i$; for sinusoidally distributed thermal load (25a)

$T_{mn}^{i} = \dfrac{16\hat{T}_i}{rs\pi^2}$; for uniformly distributed thermal load (25b)

From Equation (19a-i), it can be noticed that for N_i, M_i, P_i, Q_i, K_i, and R_i, the variables depending on x and y are the strains, ε_j^b (b=0,…,5). Therefore, the expressions in each of the plate governing Equations (18a-f), for example $\dfrac{\partial^2 N_i}{\partial x^2}$, $\dfrac{\partial^2 M_i}{\partial x^2}$, can be expressed as follows:

$$\frac{\partial^2 (N_i, M_i)}{\partial x^2} = (A_{ij}, B_{ij}) \begin{bmatrix} \begin{bmatrix} \lambda^3 & 0 & 0 & 0 & 0 & 0 \\ 0 & \lambda^2\beta & 0 & 0 & 0 & 0 \\ 0 & 0 & 0 & 0 & 0 & 0 \\ 0 & 0 & 0 & 0 & -y^*\lambda^2 & -q^*\lambda^2\beta \\ 0 & 0 & 0 & -y^*\lambda^2 & 0 & -q^*\lambda^3 \\ -\lambda^2\beta & -\lambda^3 & 0 & 0 & 0 & 0 \end{bmatrix} \begin{bmatrix} U_{rs} \\ V_{rs} \\ W_{rs} \\ \Theta_{rs}^1 \\ \Theta_{rs}^2 \\ \Theta_{rs}^3 \end{bmatrix}^T \end{bmatrix} \times \begin{Bmatrix} SS \\ SS \\ SS \\ SC \\ CS \\ CC \end{Bmatrix} +$$

$$(B_{ij}, G_{ij}) \begin{bmatrix} \begin{bmatrix} 0 & 0 & -\lambda^4 & y^*\lambda^3 & 0 & q^*\lambda^4 \\ 0 & 0 & -\lambda^2\beta^2 & 0 & y^*\lambda^2\beta & q^*\lambda^2\beta^2 \\ 0 & 0 & 0 & 0 & 0 & 0 \\ 0 & 0 & 0 & 0 & 0 & 0 \\ 0 & 0 & 0 & 0 & 0 & 0 \\ 0 & 0 & 2\lambda^3\beta & -y^*\lambda^2\beta & -y^*\lambda^3 & -2q^*\lambda^3\beta \end{bmatrix} \begin{bmatrix} U_{rs} \\ V_{rs} \\ W_{rs} \\ \Theta_{rs}^1 \\ \Theta_{rs}^2 \\ \Theta_{rs}^3 \end{bmatrix}^T \end{bmatrix} \times \begin{Bmatrix} SS \\ SS \\ SS \\ SC \\ CS \\ CC \end{Bmatrix} +$$

$$(C_{ij}, H_{ij}) \begin{bmatrix} \begin{bmatrix} 0 & 0 & 0 & \lambda^3 & 0 & 0 \\ 0 & 0 & 0 & 0 & \lambda^2\beta & 0 \\ 0 & 0 & 0 & 0 & 0 & 0 \\ 0 & 0 & 0 & 0 & 0 & 0 \\ 0 & 0 & 0 & 0 & 0 & 0 \\ 0 & 0 & 0 & -\lambda^2\beta & -\lambda^3 & 0 \end{bmatrix} \begin{bmatrix} U_{rs} \\ V_{rs} \\ W_{rs} \\ \Theta_{rs}^1 \\ \Theta_{rs}^2 \\ \Theta_{rs}^3 \end{bmatrix}^T \end{bmatrix} \times \begin{Bmatrix} SS \\ SS \\ SS \\ SC \\ CS \\ CC \end{Bmatrix} +$$

$$(D_{ij},I_{ij})\left[\begin{bmatrix} 0 & 0 & 0 & 0 & 0 & 0 \\ 0 & 0 & 0 & 0 & 0 & 0 \\ 0 & 0 & 0 & 0 & 0 & 0 \\ 0 & 0 & 0 & 0 & 0 & -\lambda^2\beta \\ 0 & 0 & 0 & 0 & 0 & -\lambda^3 \\ 0 & 0 & 0 & 0 & 0 & 0 \end{bmatrix}\begin{bmatrix} U_{rs} \\ V_{rs} \\ W_{rs} \\ \Theta^1_{rs} \\ \Theta^2_{rs} \\ \Theta^3_{rs} \end{bmatrix}^T \times \begin{Bmatrix} SS \\ SS \\ SS \\ SC \\ CS \\ CC \end{Bmatrix} + \right.$$

$$(E_{ij},J_{ij})\left[\begin{bmatrix} 0 & 0 & 0 & 0 & 0 & 0 \\ 0 & 0 & 0 & 0 & 0 & 0 \\ 0 & 0 & 0 & 0 & 0 & 0 \\ 0 & 0 & 0 & 0 & -\lambda^2 & 0 \\ 0 & 0 & 0 & -\lambda^2 & 0 & 0 \\ 0 & 0 & 0 & 0 & 0 & 0 \end{bmatrix}\begin{bmatrix} U_{rs} \\ V_{rs} \\ W_{rs} \\ \Theta^1_{rs} \\ \Theta^2_{rs} \\ \Theta^3_{rs} \end{bmatrix}^T \times \begin{Bmatrix} SS \\ SS \\ SS \\ SC \\ CS \\ CC \end{Bmatrix} + \right.$$

$$(F_{ij},K'_{ij})\left[\begin{bmatrix} 0 & 0 & 0 & 0 & 0 & 0 \\ 0 & 0 & 0 & 0 & 0 & 0 \\ 0 & 0 & 0 & 0 & 0 & -\lambda^2 \\ 0 & 0 & 0 & 0 & 0 & 0 \\ 0 & 0 & 0 & 0 & 0 & 0 \\ 0 & 0 & 0 & 0 & 0 & 0 \end{bmatrix}\begin{bmatrix} U_{rs} \\ V_{rs} \\ W_{rs} \\ \Theta^1_{rs} \\ \Theta^2_{rs} \\ \Theta^3_{rs} \end{bmatrix}^T \times \begin{Bmatrix} SS \\ SS \\ SS \\ SC \\ CS \\ CC \end{Bmatrix} - \frac{\partial^2 (N_i^T, M_i^T)}{\partial x^2}. \right. \qquad (26)$$

where $SS = \sin(\lambda x)\sin(\beta y)$, $SC = \sin(\lambda x)\cos(\beta y)$ and so for, and the elements of the 6x6 matrices are the coefficients obtained after taking the second derivation of the strains expression in the Equations (19a-i). As is known, the generalized strains are expressions as a function of the 6 unknowns, described in Equations (3a-c) and Equations (22a-f).

The 6x6 matrices associated with $\frac{\partial^2 M_i}{\partial x^2}$ in Equation (26), is called $\overline{M}_x^{2,b}$ (b=0,…,5). The symbols used in $\overline{M}_v^{a,b}$ are as follow: the first upper and lower (a,v) indicates the derivative (second derivative with respect to x, in the example), and the second upper character, b, indicates that the derivative is associates with the strain ε_j^b (b=0,…,5). For example, $\overline{M}_x^{2,0}$ is (see Equation (26)):

$$\overline{M}_x^{2,0}=\begin{bmatrix} \lambda^3 & 0 & 0 & 0 & 0 & 0 \\ 0 & \lambda^2\beta & 0 & 0 & 0 & 0 \\ 0 & 0 & 0 & 0 & 0 & 0 \\ 0 & 0 & 0 & 0 & -y^*\lambda^2 & -q^*\lambda^2\beta \\ 0 & 0 & 0 & -y^*\lambda^2 & 0 & -q^*\lambda^3 \\ -\lambda^2\beta & -\lambda^3 & 0 & 0 & 0 & 0 \end{bmatrix} \tag{27}$$

By collecting the expression obtained after substituting Equations (22a-f) and (24) into Equations (18a-f), the following equation is obtained,

$$K_{ij}\Delta_j = \{F\} \qquad (i, j = 1,.....,6) \text{ and } (K_{ij} = K_{ji}). \tag{28}$$

where Δ_j is the column vector of coefficients $\{U_{rs}\ V_{rs}\ W_{rs}^b\ \Theta_{rs}^1\ \Theta_{rs}^2\ \Theta_{rs}^3\}$ and $\{F\}=\{F_1\ \ F_2\ \ F_3\ \ F_4\ \ F_5\ \ F_6\}^T$ is the column vector of coefficients of the thermal load:

$$F_1 = \lambda\left(\mathrm{A}_{1\mathrm{j}}^*\hat{T}_1 + \mathrm{B}_{1\mathrm{j}}^*\frac{\hat{T}_2}{h} + \mathrm{C}_{1\mathrm{j}}^*\frac{\hat{T}_3}{h}\right)\{T^u\} \tag{29a}$$

$$F_2 = \beta\left(\mathrm{A}_{2\mathrm{j}}^*\hat{T}_1 + \mathrm{B}_{2\mathrm{j}}^*\frac{\hat{T}_2}{h} + \mathrm{C}_{2\mathrm{j}}^*\frac{\hat{T}_3}{h}\right)\{T^u\} \tag{29b}$$

$$F_3 = -\lambda^2\left(\mathrm{B}_{1\mathrm{j}}^*\hat{T}_1 + \mathrm{G}_{1\mathrm{j}}^*\frac{\hat{T}_2}{h} + \mathrm{H}_{1\mathrm{j}}^*\frac{\hat{T}_3}{h}\right)\{T^u\} - \beta^2\left(\mathrm{B}_{2\mathrm{j}}^*\hat{T}_1 + \mathrm{G}_{2\mathrm{j}}^*\frac{\hat{T}_2}{h} + \mathrm{H}_{2\mathrm{j}}^*\frac{\hat{T}_3}{h}\right)\{T^u\} \tag{29c}$$

$$F_4 = y^*\lambda\left(\mathrm{B}_{1\mathrm{j}}^*\hat{T}_1 + \mathrm{G}_{1\mathrm{j}}^*\frac{\hat{T}_2}{h} + \mathrm{H}_{1\mathrm{j}}^*\frac{\hat{T}_3}{h}\right)\{T^u\} + \lambda\left(\mathrm{C}_{1\mathrm{j}}^{**}\hat{T}_1 + \mathrm{H}_{1\mathrm{j}}^{**}\frac{\hat{T}_2}{h} + \mathrm{L}_{1\mathrm{j}}^{**}\frac{\hat{T}_3}{h}\right)\{T^u\} \tag{29d}$$

$$F_5 = y^*\beta\left(\mathrm{B}_{2\mathrm{j}}^*\hat{T}_1 + \mathrm{G}_{2\mathrm{j}}^*\frac{\hat{T}_2}{h} + \mathrm{H}_{2\mathrm{j}}^*\frac{\hat{T}_3}{h}\right)\{T^u\} + \beta\left(\mathrm{C}_{2\mathrm{j}}^{**}\hat{T}_1 + \mathrm{H}_{2\mathrm{j}}^{**}\frac{\hat{T}_2}{h} + \mathrm{L}_{2\mathrm{j}}^{**}\frac{\hat{T}_3}{h}\right)\{T^u\} \tag{29e}$$

$$F_6 = q^*\lambda^2\left(\mathrm{B}_{1\mathrm{j}}^*\hat{T}_1 + \mathrm{G}_{1\mathrm{j}}^*\frac{\hat{T}_2}{h} + \mathrm{H}_{1\mathrm{j}}^*\frac{\hat{T}_3}{h}\right)\{T^u\} + q^*\beta^2\left(\mathrm{B}_{2\mathrm{j}}^*\hat{T}_1 + \mathrm{G}_{2\mathrm{j}}^*\frac{\hat{T}_2}{h} + \mathrm{H}_{2\mathrm{j}}^*\frac{\hat{T}_3}{h}\right)\{T^u\}$$

$$-\left(\mathrm{F}_{3\mathrm{j}}^{*}\hat{T}_1+\mathrm{K}'^{*}_{3\mathrm{j}}\frac{\hat{T}_2}{h}+\mathrm{O}_{3\mathrm{j}}^{*}\frac{\hat{T}_3}{h}\right)\left\{T^u\right\} \tag{29f}$$

$$\left\{T^u\right\}=\left\{1\quad 1\quad 1\quad 0\quad 0\quad 0\right\}^T \tag{29g}$$

Elements of K_{ij} in Equation (28) can be obtained by using the matrices $\overline{M}_v^{a,b}$. All matrices of type $\overline{M}_v^{a,b}$, associated with the expressions of the plate governing Equations (18a-f) are given in Appendix A.

4. Numerical results and discussions

In this section, the results of thermoelastic bending analysis of FG sandwich plates by using the present theory are presented. As it was mentioned above, this theory includes the thickness stretching effect, i.e. the thickness expansion is well-modeled, obeying the Koiter's recommendation regarding the thickness stretching effect of the plate [3]. Therefore, in order to evaluate this theory various numerical examples of a FG sandwich plate with various exponents that specify the material variation profile through the thickness, "*p*", several aspect ratio "a/b" and different schemes are presented. Typical mechanical properties for metal and ceramics used in the numerical examples are listed in Table 1. The simply supported FG sandwich plate is subjected to a bi-sinusoidal thermal load. All results were obtained considering a side-to-thickness ratio a/h=10. In this paper, the following dimensionless relations for the deflection and stresses of thermoelastic bending problem are used:

$$\overline{w}=\frac{h}{\alpha_0\hat{T}_2a^2}w\left(\frac{a}{2},\frac{b}{2}\right),\ \overline{\sigma}_{xx}=\frac{h^2}{\alpha_0\hat{T}_2E_0a^2}\sigma_{xx}\left(\frac{a}{2},\frac{b}{2},\frac{h}{2}\right),\ \overline{\tau}_{xz}=\frac{10h}{\alpha_0\hat{T}_2E_0a}\tau_{xz}\left(0,\frac{b}{2},0\right)$$

$$E_0=1GPa,\ \alpha_0=10^{-6}{}^{\circ}C^{-1} \tag{28}$$

The results of non-dimensional deflections w of FG sandwich square plates for several values of exponent "*p*" and different sandwich schemes are presented in Table 2. The sandwich plate is subjected to a linear temperature distribution through the thickness ($\hat{T}_3=0$). The results are compared with solutions based on TSDT and HSDTs with thickness stretching effect proposed by Zenkour and Alghamdi [5] and Houari et al. [13]. From Table 2 can be

noticed that the present results show excellent agreement with other HSDTs with thickness stretching effect [5,13]. It can be also noticed that theories with thickness stretching effect (including the present one) presents lower non-dimensional deflection results than other solutions based on classical 2D HSDTs ($\varepsilon_{zz} = 0$). For a given sandwich scheme, the non-dimensional deflection increases as the exponent "*p*" increases. However, this effect decreases for high values of the exponent "*p*".

Table 3 presents results of non-dimensional deflections w of FG sandwich plates for different values of aspect ratio "a/b" and several sandwich schemes, considering the exponent *p*=3. As before, the sandwich plate is subjected to a linear temperature distribution through the thickness ($\hat{T}_3 = 0$). The results are compared with several HSDTs as in Table 2. The results of the present theory show excellent agreement with other theories with thickness stretching effect, as expected. For a given sandwich scheme, the non-dimensional deflection decreases as the aspect ratio "a/b" increases. It can be noticed that the present results are lower than the solutions based on classical 2D HSDTs. However, this pattern is opposite for aspect ratios a/b > 3. From Tables 2 and 3, it can be said that the aspect ratio "a/b" is more influential in non-dimensional deflection than the exponent "*p*".

Results of non-dimensional axial stresses $\bar{\sigma}_{xx}$ of FG sandwich square plates for several values of exponent "*p*" and different sandwich schemes are presented in Table 4. The sandwich plate is subjected to a linear temperature distribution through the thickness ($\hat{T}_3 = 0$). Again, the present results show an excellent agreement with other solutions with thickness stretching effect. The present results are higher (in absolute value) than the other solutions based on theories that consider $\varepsilon_{zz} = 0$. From this table can be seen that the non-dimensional axial stress decrease as the exponent "*p*" increase, except for the exponent *p*=0.

Table 5 presents results of non-dimensional transverse shear stresses $\bar{\tau}_{xz}$ of FG sandwich square plates for several values of exponent "*p*" and different sandwich schemes. The results are compared with several HSDTs as mentioned previously. The sandwich plate is subjected to both linear and nonlinear temperature distribution ($\hat{T}_3 = -100$). Note that this table was prepared by considering that the function of the nonlinear temperature distribution is equal to shear strain shape function of the displacement field, i.e., $f(z) = \Psi(z)$. It can be noticed that the results of all theories are different, except the solutions based on HSDTs with

thickness stretching effect proposed by Zenkour and Alghamdi [5] and Houari et al. [13] (both theories presented a non-linear temperature field with a sine function). The difference in results is attributed to the nonlinear term of the temperature field.

Due to the capability of the present generalized theory, Table 6 presents a comparison of the non-dimensional transverse shear stresses $\bar{\tau}_{xz}$ considering a generalized temperature distribution through the thickness ($f(z) \neq \Psi(z)$). Interestingly, it can be noticed that the results are different in all cases. It is worth highlighting that the temperature field with polynomial function produces lower values of transverse shear stress.

Figures 3 and 4 show the variation of the non-dimensional deflection $\bar{w}$ as a function of the exponent "*p*" and the aspect ratio "a/b" for various values of the coefficient of thermal load $\hat{T}_3$, respectively. The nonlinear term of the temperature distribution presents a sinusoidal function, i.e. $\Psi(z) = (h/\pi)\sin(\pi z/h)$. In Figure 3 (for a certain value of $\hat{T}_3$) can be seen that the non-dimensional deflection remains practically constant for high values of the exponent "*p*". The non-dimensional deflection increases as the coefficient of thermal load $\hat{T}_3$ increases. Figure 4 shows that the curves have negative slope, i.e. the non-dimensional deflection decreases as the aspect ratio "a/b" increases, and as "a/b" is reduced the non-dimensinalized deflections are higher. However, the effect decreases as $\hat{T}_3$ decreases. From Figures 3 and 4 can be clearly seen that the aspect ratio has a greater influence on the deflection than the exponent "*p*".

Figures 5 and 6 show the distribution of the non-dimensional deflections, $\bar{w}$, and the axial stresses, $\bar{\sigma}_{xx}$, through the thickness of the plate for several exponents "*p*", respectively. The sandwich plate is subjected to linear temperature distribution ($\hat{T}_3 = 0$). From Figure 5 can be noticed that the non-dimensional deflection has its maximum value on the plate surfaces. The non-dimensional deflection increases as the exponent "*p*" increases. As in the non-dimensional deflection, the non-dimensional axial stress reaches its maximum value on the plate surfaces (see Figure 6).

Figures 7 and 8 show the variation of the deflection w as a function of the coefficient of thermal load $\hat{T}_2$ for several values of $\hat{T}_1$ and $\hat{T}_3$, respectively. From Figure 7 can be

observed that the coefficient of thermal load $\hat{T}_1$ has no influence on the results. However, the coefficient of thermal load $\hat{T}_3$ significantly affects the deflection, see Figure 8.

The distribution of the non-dimensional deflection, axial stress and transverse shear stress through the thickness of the plate for several coefficients of thermal load $\hat{T}_3$ are shown in Figures 9, 10 and 11, respectively. From these figures can be concluded that the results are very sensitive to the coefficient of thermal load $\hat{T}_3$.

5. Conclusions

This paper presents a thermoelastic bending analysis for a FG sandwich plate by using of a new quasi-3D hybrid type HSDT subjected to a generalized temperature field. Many hybrid types of shear deformation theories with only 6 unknowns, in which the thickness stretching effect is included, can be derived by using the present generalized formulation. The nonlinear term of the temperature can be different from the shear strain shape functions of the displacement field. The governing equations are obtained through the principle of virtual work. These equations are solved via Navier's method. The results were compared with the solutions of several theories. It is concluded that the results of the present theory has an excellent agreement with other theories with thickness stretching effect for the thermoelastic bending problem. The non-dimensional stresses σ_{xx}, τ_{xz} and non-dimensional deflection w are sensitive to the nonlinear term of the temperature field. Furthermore, the nature of the nonlinear term of the temperature field (polynomial, sinusoidal, tangential, or other) highly affects the results of the non-dimensional deflection and stresses. Consequently, it should be extensively discussed in futures research works due to limited comments about it in the scientific community.

Acknowledgment

This work has been performed due to the opportunity, confidence and special support of the following Persons: Carlos Heeren, Alberto Bejarano, Enrique Sarmiento and Alexander Peralta.

Appendix A. Definition of constants in Equation (28)

As mentioned before, these matrices are associated with the expressions of the plate governing Equations (18a-f) they used to calculate the Kij element matrices. The advantage of the present technique is that infinite shear deformation theories can be created and calculated by using the same following matrices, only "y*" and "q*" should be changed.

$$\overline{M}^{0,0}=\begin{bmatrix} -\lambda & 0 & 0 & 0 & 0 & 0 \\ 0 & -\beta & 0 & 0 & 0 & 0 \\ 0 & 0 & 0 & 0 & 0 & 0 \\ 0 & 0 & 0 & 0 & y^* & q^*\beta \\ 0 & 0 & 0 & y^* & 0 & q^*\lambda \\ \beta & \lambda & 0 & 0 & 0 & 0 \end{bmatrix}, \quad \overline{M}^{0,1}=\begin{bmatrix} 0 & 0 & \lambda^2 & -y^*\lambda & 0 & -q^*\lambda^2 \\ 0 & 0 & \beta^2 & 0 & -y^*\beta & -q^*\beta^2 \\ 0 & 0 & 0 & 0 & 0 & 0 \\ 0 & 0 & 0 & 0 & 0 & 0 \\ 0 & 0 & 0 & 0 & 0 & 0 \\ 0 & 0 & -2\lambda\beta & y^*\beta & y^*\lambda & 2q^*\lambda\beta \end{bmatrix}$$

$$\overline{M}^{0,2}=\begin{bmatrix} 0 & 0 & 0 & -\lambda & 0 & 0 \\ 0 & 0 & 0 & 0 & -\beta & 0 \\ 0 & 0 & 0 & 0 & 0 & 0 \\ 0 & 0 & 0 & 0 & 0 & 0 \\ 0 & 0 & 0 & 0 & 0 & 0 \\ 0 & 0 & 0 & \beta & \lambda & 0 \end{bmatrix}, \quad \overline{M}^{0,3}=\begin{bmatrix} 0 & 0 & 0 & 0 & 0 & 0 \\ 0 & 0 & 0 & 0 & 0 & 0 \\ 0 & 0 & 0 & 0 & 0 & 0 \\ 0 & 0 & 0 & 0 & 0 & \beta \\ 0 & 0 & 0 & 0 & 0 & \lambda \\ 0 & 0 & 0 & 0 & 0 & 0 \end{bmatrix}$$

$$\overline{M}^{0,4}=\begin{bmatrix} 0 & 0 & 0 & 0 & 0 & 0 \\ 0 & 0 & 0 & 0 & 0 & 0 \\ 0 & 0 & 0 & 0 & 0 & 0 \\ 0 & 0 & 0 & 0 & 1 & 0 \\ 0 & 0 & 0 & 1 & 0 & 0 \\ 0 & 0 & 0 & 0 & 0 & 0 \end{bmatrix}, \quad \overline{M}^{0,5}=\begin{bmatrix} 0 & 0 & 0 & 0 & 0 & 0 \\ 0 & 0 & 0 & 0 & 0 & 0 \\ 0 & 0 & 0 & 0 & 0 & 1 \\ 0 & 0 & 0 & 0 & 0 & 0 \\ 0 & 0 & 0 & 0 & 0 & 0 \\ 0 & 0 & 0 & 0 & 0 & 0 \end{bmatrix}$$

$$\overline{M}_x^{1,0}=\begin{bmatrix} -\lambda^2 & 0 & 0 & 0 & 0 & 0 \\ 0 & -\lambda\beta & 0 & 0 & 0 & 0 \\ 0 & 0 & 0 & 0 & 0 & 0 \\ 0 & 0 & 0 & 0 & y^*\lambda & q^*\lambda\beta \\ 0 & 0 & 0 & -y^*\lambda & 0 & -q^*\lambda^2 \\ -\lambda\beta & -\lambda^2 & 0 & 0 & 0 & 0 \end{bmatrix},$$

$$\overline{M}_x^{1,1}=\begin{bmatrix}0&0&\lambda^3&-y^*\lambda^2&0&-q^*\lambda^3\\0&0&\lambda\beta^2&0&-y^*\lambda\beta&-q^*\lambda\beta^2\\0&0&0&0&0&0\\0&0&0&0&0&0\\0&0&0&0&0&0\\0&0&2\lambda^2\beta&-y^*\lambda\beta&-y^*\lambda^2&-2q^*\lambda^2\beta\end{bmatrix}$$

$$\overline{M}_x^{1,2}=\begin{bmatrix}0&0&0&-\lambda^2&0&0\\0&0&0&0&-\lambda\beta&0\\0&0&0&0&0&0\\0&0&0&0&0&0\\0&0&0&0&0&0\\0&0&0&-\lambda\beta&-\lambda^2&0\end{bmatrix},\qquad \overline{M}_x^{1,3}=\begin{bmatrix}0&0&0&0&0&0\\0&0&0&0&0&0\\0&0&0&0&0&0\\0&0&0&0&0&\lambda\beta\\0&0&0&0&0&-\lambda^2\\0&0&0&0&0&0\end{bmatrix}$$

$$\overline{M}_x^{1,4}=\begin{bmatrix}0&0&0&0&0&0\\0&0&0&0&0&0\\0&0&0&0&0&0\\0&0&0&0&\lambda&0\\0&0&0&-\lambda&0&0\\0&0&0&0&0&0\end{bmatrix},\qquad \overline{M}_x^{1,5}=\begin{bmatrix}0&0&0&0&0&0\\0&0&0&0&0&0\\0&0&0&0&0&\lambda\\0&0&0&0&0&0\\0&0&0&0&0&0\\0&0&0&0&0&0\end{bmatrix}$$

$$\overline{M}_y^{1,0}=\begin{bmatrix}-\lambda\beta&0&0&0&0&0\\0&-\beta^2&0&0&0&0\\0&0&0&0&0&0\\0&0&0&0&-y^*\beta&-q^*\beta^2\\0&0&0&y^*\beta&0&q^*\lambda\beta\\-\beta^2&-\lambda\beta&0&0&0&0\end{bmatrix},\ \overline{M}_y^{1,1}=\begin{bmatrix}0&0&\lambda^2\beta&-y^*\lambda\beta&0&-q^*\lambda^2\beta\\0&0&\beta^3&0&-y^*\beta^2&-q^*\beta^3\\0&0&0&0&0&0\\0&0&0&0&0&0\\0&0&0&0&0&0\\0&0&2\lambda\beta^2&-y^*\beta^2&-y^*\lambda\beta&-2q^*\lambda\beta^2\end{bmatrix}$$

$$\overline{M}_y^{1,2}=\begin{bmatrix}0&0&0&-\lambda\beta&0&0\\0&0&0&0&-\beta^2&0\\0&0&0&0&0&0\\0&0&0&0&0&0\\0&0&0&0&0&0\\0&0&0&-\beta^2&-\lambda\beta&0\end{bmatrix},\qquad \overline{M}_y^{1,3}=\begin{bmatrix}0&0&0&0&0&0\\0&0&0&0&0&0\\0&0&0&0&0&0\\0&0&0&0&0&-\beta^2\\0&0&0&0&0&\lambda\beta\\0&0&0&0&0&0\end{bmatrix}$$

$$\overline{M}_y^{1,4}=\begin{bmatrix}0&0&0&0&0&0\\0&0&0&0&0&0\\0&0&0&0&0&0\\0&0&0&0&-\beta&0\\0&0&0&\beta&0&0\\0&0&0&0&0&0\end{bmatrix},\qquad \overline{M}_y^{1,5}=\begin{bmatrix}0&0&0&0&0&0\\0&0&0&0&0&0\\0&0&0&0&0&\beta\\0&0&0&0&0&0\\0&0&0&0&0&0\\0&0&0&0&0&0\end{bmatrix}$$

$$\overline{M}_y^{2,0}=\begin{bmatrix}\lambda\beta^2&0&0&0&0&0\\0&\beta^3&0&0&0&0\\0&0&0&0&0&0\\0&0&0&0&-y^*\beta^2&-q^*\beta^3\\0&0&0&-y^*\beta^2&0&-q^*\lambda\beta^2\\-\beta^3&-\lambda\beta^2&0&0&0&0\end{bmatrix},$$

$$\overline{M}_y^{2,1}=\begin{bmatrix}0&0&-\lambda^2\beta^2&y^*\lambda\beta^2&0&q^*\lambda^2\beta^2\\0&0&-\beta^4&0&y^*\beta^3&q^*\beta^4\\0&0&0&0&0&0\\0&0&0&0&0&0\\0&0&0&0&0&0\\0&0&2\lambda\beta^3&-y^*\beta^3&-y^*\lambda\beta^2&-2q^*\lambda\beta^3\end{bmatrix}$$

$$\overline{M}_y^{2,2}=\begin{bmatrix}0&0&0&\lambda\beta^2&0&0\\0&0&0&0&\beta^3&0\\0&0&0&0&0&0\\0&0&0&0&0&0\\0&0&0&0&0&0\\0&0&0&-\beta^3&-\lambda\beta^2&0\end{bmatrix},\qquad \overline{M}_y^{2,3}=\begin{bmatrix}0&0&0&0&0&0\\0&0&0&0&0&0\\0&0&0&0&0&0\\0&0&0&0&0&-\beta^3\\0&0&0&0&0&-\lambda\beta^2\\0&0&0&0&0&0\end{bmatrix}$$

$$\overline{M}_y^{2,4}=\begin{bmatrix}0&0&0&0&0&0\\0&0&0&0&0&0\\0&0&0&0&0&0\\0&0&0&0&-\beta^2&0\\0&0&0&-\beta^2&0&0\\0&0&0&0&0&0\end{bmatrix},\qquad \overline{M}_y^{2,5}=\begin{bmatrix}0&0&0&0&0&0\\0&0&0&0&0&0\\0&0&0&0&0&-\beta^2\\0&0&0&0&0&0\\0&0&0&0&0&0\\0&0&0&0&0&0\end{bmatrix}$$

$$\overline{M}_{xy}^{2,0}=\begin{bmatrix}-\lambda^2\beta&0&0&0&0&0\\0&-\lambda\beta^2&0&0&0&0\\0&0&0&0&0&0\\0&0&0&0&-y^*\lambda\beta&-q^*\lambda\beta^2\\0&0&0&-y^*\lambda\beta&0&-q^*\lambda^2\beta\\\lambda\beta^2&\lambda^2\beta&0&0&0&0\end{bmatrix},$$

$$\overline{M}_{xy}^{2,1}=\begin{bmatrix} 0 & 0 & \alpha^3\beta & -y^*\alpha^2\beta & 0 & -q^*\alpha^3\beta \\ 0 & 0 & \alpha\beta^3 & 0 & -y^*\alpha\beta^2 & -q^*\alpha\beta^3 \\ 0 & 0 & 0 & 0 & 0 & 0 \\ 0 & 0 & 0 & 0 & 0 & 0 \\ 0 & 0 & 0 & 0 & 0 & 0 \\ 0 & 0 & -2\alpha^2\beta^2 & y^*\alpha\beta^2 & y^*\alpha^2\beta & 2q^*\alpha^2\beta^2 \end{bmatrix}$$

$$\overline{M}_{xy}^{2,2}=\begin{bmatrix} 0 & 0 & 0 & -\lambda^2\beta & 0 & 0 \\ 0 & 0 & 0 & 0 & -\lambda\beta^2 & 0 \\ 0 & 0 & 0 & 0 & 0 & 0 \\ 0 & 0 & 0 & 0 & 0 & 0 \\ 0 & 0 & 0 & 0 & 0 & 0 \\ 0 & 0 & 0 & \lambda\beta^2 & \lambda^2\beta & 0 \end{bmatrix},\qquad \overline{M}_{xy}^{2,3}=\begin{bmatrix} 0 & 0 & 0 & 0 & 0 & 0 \\ 0 & 0 & 0 & 0 & 0 & 0 \\ 0 & 0 & 0 & 0 & 0 & 0 \\ 0 & 0 & 0 & 0 & 0 & -\lambda\beta^2 \\ 0 & 0 & 0 & 0 & 0 & -\lambda^2\beta \\ 0 & 0 & 0 & 0 & 0 & 0 \end{bmatrix}$$

$$\overline{M}_{xy}^{2,4}=\begin{bmatrix} 0 & 0 & 0 & 0 & 0 & 0 \\ 0 & 0 & 0 & 0 & 0 & 0 \\ 0 & 0 & 0 & 0 & 0 & 0 \\ 0 & 0 & 0 & 0 & -\lambda\beta & 0 \\ 0 & 0 & 0 & -\lambda\beta & 0 & 0 \\ 0 & 0 & 0 & 0 & 0 & 0 \end{bmatrix},\qquad \overline{M}_{xy}^{2,5}=\begin{bmatrix} 0 & 0 & 0 & 0 & 0 & 0 \\ 0 & 0 & 0 & 0 & 0 & 0 \\ 0 & 0 & 0 & 0 & 0 & \lambda\beta \\ 0 & 0 & 0 & 0 & 0 & 0 \\ 0 & 0 & 0 & 0 & 0 & 0 \\ 0 & 0 & 0 & 0 & 0 & 0 \end{bmatrix}$$

References

1. M.B. Bever, P.E. Duwez, Gradients in composite materials. Materials Science and Engineering 1972;10:1-8.
2. Koizumi M. The concept of FGM. Ceramic transactions. Funct Grad Mater 1993;34:3-10.
3. Koiter WT. A consistent first approximation in the general theory of thin elastic shells. In: Proceedings of first symposium on the theory of thin elastic shells. Amsterdam: North-Holland; 1959.
4. Zenkour AM. Benchmark trigonometric and 3-D elasticity solutions for an exponentially graded thick rectangular plate. Appl Math Model 2007;77:197-214.
5. Zenkour AM, Alghamdi NA. Thermoelastic bending analysis of functionally graded sandwich plates. J Mater Sci 2008;43:2574-89.

6. Matsunaga H. Stress analysis of functionally graded plates subjected to thermal and mechanical loadings. Compos Struct 2009;87:344-57.
7. Carrera E, Brischetto S, Cinefra M, Soave M. Effects of thickness stretching in functionally graded plates and shells. Composites: Part B 2011;42:123-33.
8. Neves AMA, Ferreira AJM, Carrera E, Roque CMC, Cinefra M, Jorge RMN, et al. A quasi-3D sinusoidal shear deformation theory for the static and free vibration analysis of functionally graded plates. Composites: Part B 2012;43:711-25.
9. Neves AMA, Ferreira AJM, Carrera E, Cinefra M, Roque CMC, Jorge RMN, et al. A quasi-3D hyperbolic shear deformation theory for the static and free vibration analysis of functionally graded plates. Composites: Part B 2012;94:1814-25.
10. Mantari JL, Guedes Soares C. Generalized hybrid quasi-3D shear deformation theory for the static analysis of advanced composite plates. Compos Struct 2012;94:2561-75.
11. Mantari JL, Guedes Soares C. A novel higher-order shear deformation theory with stretching effect for functionally graded plates. Composites: Part B 2013;45:268-81.
12. Mantari JL, Guedes Soares C. A trigonometric plate theory with 5-unknowns and stretching effect for advanced composite plates. Compos Struct 2014;107:396-405.
13. Houari MSA, Tounsi A, Anwar Bég O. Thermoelastic bending analysis of functionally graded sandwich plates using a new higher order shear and normal deformation theory. Int J Mech Sci 2013;76:102-11.
14. H Saidi, MSA Houari, A Tounsi, EAA Bedia. Thermo-mechanical bending response with stretching effect of functionally graded sandwich plates using a novel shear deformation theory. Steel and Composite Structures 2013;15:221-245.
15. Ait Amar Meziane M, Abdelaziz HH, Tounsi A. An efficient and simple refined theory for buckling and free vibration of exponentially graded sandwich plates under various boundary conditions. Journal of Sandwich Structures and Materials 2014;16(3):293 – 318.
16. Bouderba B, Houari MSA, Tounsi A. Thermomechanical bending response of FGM thick plates resting on Winkler–Pasternak elastic foundations. Steel and Composite Structures 2015;14(1):85-104.

17. Zidi M, Tounsi A, Houari MSA, Adda Bedia EA, Anwar Bég O. Bending analysis of FGM plates under hygro-thermo-mechanical loading using a four variable refined plate theory. Aerospace Science and Technology 2014;34:24–34.

Table Legends

Table 1. Material properties of the used FG sandwich plates.

Table 2. Comparison of non-dimensional deflection $\overline{w}$ of FG sandwich square plates (a/h=10, $\hat{T}_1 = \hat{T}_3 = 0$, $\hat{T}_2 = 100$).

Table 3. Comparison of non-dimensional deflection $\overline{w}$ of FG sandwich rectangular plates (*p*=3, a/h=10, $\hat{T}_1 = \hat{T}_3 = 0$, $\hat{T}_2 = 100$).

Table 4. Comparison of non-dimensional axial stress σ_{xx} of FG sandwich plates (a/h=10, $\hat{T}_1 = \hat{T}_3 = 0$, $\hat{T}_2 = 100$).

Table 5. Comparison of non-dimensional shear stress τ_{xz} of FG sandwich square plates (a/h=10, $\hat{T}_1 = 0$, $\hat{T}_2 = 100$, $\hat{T}_3 = -100$, $f(z) = \Psi(z)$).

Table 6. Comparison of non-dimensional shear stress τ_{xz} of FG sandwich square plates (a/h=10, $\hat{T}_1 = 0$, $\hat{T}_2 = 100$, $\hat{T}_3 = -100$, $f(z) \neq \Psi(z)$).

Figure Captions

Figure 1. Geometry of functionally graded sandwich plate.

Figure 2. Volume fraction for the ceramic phase, $V_{(z)}$, along the thickness of a FGP for different values of the exponent "*p*" (1-2-1).

Figure 3. Variation of non-dimensional deflection w of FG sandwich square plate versus the exponent "*p*" considering a generalized temperature field with a sine function ($\hat{T}_1 = 0$, $\hat{T}_2 = 100$, a/h = 10, 1-1-1, $\Psi(z) = (h/\pi)\sin(\pi z/h)$).

Figure 4. Variation of non-dimensional deflection w of FG sandwich plate versus the aspect ratio "a/b" considering a generalized temperature field with a sine function ($\hat{T}_1 = 0$, $\hat{T}_2 = 100$, a/h = 10, p=2, 1-1-1, $\Psi(z) = (h/\pi)\sin(\pi z/h)$).

Figure 5. Distribution of non-dimensional deflection w through the thickness of a FG sandwich square plate for several exponents "p" ($\hat{T}_1 = \hat{T}_3 = 0$, $\hat{T}_2 = 100$, a/h = 10, 1-1-1).

Figure 6. Distribution of non-dimensional axial stress $\bar{\sigma}_{xx}$ through the thickness of a FG sandwich square plate for several exponents "p" ($\hat{T}_1 = \hat{T}_3 = 0$, $\hat{T}_2 = 100$, a/h = 10, 1-1-1).

Figure 7. Variation of deflection w of FG sandwich square plate versus the coefficient of the thermal load $\hat{T}_2$ ($\hat{T}_3 = 0$, a/h = 10, p=2, 1-1-1).

Figure 8. Variation of deflection w of FG sandwich square plate versus the coefficient of the thermal load $\hat{T}_2$ considering a generalized temperature field with a sine function ($\Psi(z) = (h/\pi)\sin(\pi z/h)$, $\hat{T}_1 = 0$, a/h = 10, p=2, 1-1-1).

Figure 9. Distribution of non-dimensional deflection w through the thickness of a FG sandwich square plate considering a generalized temperature field with a sine function ($\Psi(z) = (h/\pi)\sin(\pi z/h)$, $\hat{T}_1 = 0$, $\hat{T}_2 = 100$, a/h = 10, p=2, 1-1-1).

Figure 10. Distribution of non-dimensional axial stress $\bar{\sigma}_{xx}$ through the thickness of a FG sandwich square plate considering a generalized temperature field with a sine function ($\Psi(z) = (h/\pi)\sin(\pi z/h)$, $\hat{T}_1 = 0$, $\hat{T}_2 = 100$, a/h = 10, p=2, 1-1-1).

Figure 11. Distribution of non-dimensional transverse shear stress $\bar{\tau}_{xz}$ through the thickness of a FG sandwich square plate considering a generalized temperature field with a sine function ($\Psi(z) = (h/\pi)\sin(\pi z/h)$, $\hat{T}_1 = 0$, $\hat{T}_2 = 100$, a/h = 10, p=2, 1-1-1).

Tables

Table 1.

Material	Properties		
	E (GPa)	**α (x10^{-6}/°C)**	**ν**
Metal: Ti–6A1–4V	66.2	10.3	1/3
Ceramic: ZrO_2	117	7.11	1/3

Table 2.

p	Theory	*w*				
		1-0-1	1-1-1	1-2-1	2-1-2	2-2-1
0	Houri et al.[13] (εz≠0)	0.461634	0.461634	0.461634	0.461634	0.461634
	Zenkour et al.[5] (εz≠0)	0.461634	0.461634	0.461634	0.461634	0.461634
	Zenkour et al.[5] (εz=0)	0.480262	0.480262	0.480262	0.480262	0.480262
	TSDT (εz=0)	0.480262	0.480262	0.480262	0.480262	0.480262
	Present (εz≠0)	**0.461630**	**0.461630**	**0.461630**	**0.461630**	**0.461630**
1	Houri et al.[13] (εz≠0)	0.614565	0.586124	0.563416	0.599933	0.573327
	Zenkour et al.[5] (εz≠0)	0.614565	0.586124	0.563416	0.599933	0.573327
	Zenkour et al.[5] (εz=0)	0.636916	0.606292	0.582342	0.621098	0.592604
	TSDT (εz=0)	0.636891	0.606256	0.582302	0.621067	0.592568
	Present (εz≠0)	**0.614560**	**0.586129**	**0.563429**	**0.599932**	**0.573335**
2	Houri et al.[13] (εz≠0)	0.647135	0.618046	0.590491	0.633340	0.601843
	Zenkour et al.[5] (εz≠0)	0.647135	0.618046	0.590491	0.633340	0.601843
	Zenkour et al.[5] (εz=0)	0.671503	0.639361	0.609875	0.656142	0.621581
	TSDT (εz=0)	0.671486	0.639325	0.609829	0.656115	0.621544
	Present (εz≠0)	**0.647118**	**0.618044**	**0.590503**	**0.633328**	**0.601847**
3	Houri et al.[13] (εz≠0)	0.658153	0.631600	0.602744	0.646475	0.614121
	Zenkour et al.[5] (εz≠0)	0.658153	0.631600	0.602744	0.646475	0.614121
	Zenkour et al.[5] (εz=0)	0.683572	0.653671	0.622467	0.670275	0.634175
	TSDT (εz=0)	0.683560	0.653638	0.622420	0.670253	0.634139
	Present (εz≠0)	**0.658131**	**0.631592**	**0.602753**	**0.646456**	**0.614121**
4	Houri et al.[13] (εz≠0)	0.662811	0.638705	0.609560	0.652890	0.620663
	Zenkour et al.[5] (εz≠0)	0.662811	0.638705	0.609560	0.652890	0.620663
	Zenkour et al.[5] (εz=0)	0.688803	0.661291	0.629533	0.677321	0.640940
	TSDT (εz=0)	0.688795	0.661260	0.629487	0.677303	0.640905
	Present (εz≠0)	**0.662785**	**0.638693**	**0.609568**	**0.652866**	**0.620661**
5	Houri et al.[13] (εz≠0)	0.665096	0.642948	0.613842	0.656490	0.624629
	Zenkour et al.[5] (εz≠0)	0.665096	0.642948	0.613842	0.656490	0.624629
	Zenkour et al.[5] (εz=0)	0.691420	0.665898	0.634003	0.681343	0.645070
	TSDT (εz=0)	0.691415	0.665869	0.633958	0.681327	0.645036
	Present (εz≠0)	**0.665071**	**0.642932**	**0.613848**	**0.656462**	**0.624625**

Table 3.

Scheme	Theory	w				
		a/b=1	a/b=2	a/b=3	a/b=4	a/b=5
1-0-1	Houri et al.[13] (εz≠0)	0.658153	0.270902	0.141810	0.088642	0.062334
	Zenkour et al.[5] (εz≠0)	0.658153	0.270902	0.141810	0.088642	0.062334
	Zenkour et al.[5] (εz=0)	0.683572	0.273492	0.136798	0.080512	0.052678
	TSDT (εz=0)	0.683560	0.273480	0.136786	0.080501	0.052667
	Present (εz≠0)	**0.658131**	**0.270879**	**0.141785**	**0.088616**	**0.062305**
1-1-1	Houri et al.[13] (εz≠0)	0.631600	0.259980	0.136105	0.085094	0.059862
	Zenkour et al.[5] (εz≠0)	0.631600	0.259980	0.136105	0.085094	0.059862
	Zenkour et al.[5] (εz=0)	0.653671	0.261647	0.130971	0.077163	0.050554
	TSDT (εz=0)	0.653638	0.261614	0.130939	0.077131	0.050522
	Present (εz≠0)	**0.631592**	**0.259972**	**0.136096**	**0.085084**	**0.059850**
1-2-1	Houri et al.[13] (εz≠0)	0.602744	0.248135	0.129933	0.081262	0.057192
	Zenkour et al.[5] (εz≠0)	0.602744	0.248135	0.129933	0.081262	0.057192
	Zenkour et al.[5] (εz=0)	0.622467	0.249245	0.124837	0.073610	0.048277
	TSDT (εz=0)	0.622420	0.249199	0.124791	0.073564	0.048231
	Present (εz≠0)	**0.602753**	**0.248144**	**0.129942**	**0.081269**	**0.057198**
2-1-2	Houri et al.[13] (εz≠0)	0.646475	0.266094	0.139295	0.087077	0.061244
	Zenkour et al.[5] (εz≠0)	0.646475	0.266094	0.139295	0.087077	0.061244
	Zenkour et al.[5] (εz=0)	0.670275	0.268228	0.134212	0.079029	0.051740
	TSDT (εz=0)	0.670253	0.268206	0.134190	0.079007	0.051718
	Present (εz≠0)	**0.646456**	**0.266074**	**0.139274**	**0.087054**	**0.061219**
2-2-1	Houri et al.[13] (εz≠0)	0.614121	0.252758	0.132303	0.082701	0.058168
	Zenkour et al.[5] (εz≠0)	0.614121	0.252758	0.132303	0.082701	0.058168
	Zenkour et al.[5] (εz=0)	0.634175	0.253878	0.127112	0.074914	0.049101
	TSDT (εz=0)	0.634139	0.253843	0.127077	0.074879	0.049066
	Present (εz≠0)	**0.614121**	**0.252758**	**0.132302**	**0.082699**	**0.058164**

Table 4.

p	Theory	$\bar{\sigma}_{xx}$				
		1-0-1	1-1-1	1-2-1	2-1-2	2-2-1
0	Houri et al.[13] (εz≠0)	-2.286893	-2.286893	-2.286893	-2.286893	-2.286893
	Zenkour et al.[5] (εz≠0)	-2.286893	-2.286893	-2.286893	-2.286893	-2.286893
	Zenkour et al.[5] (εz=0)	-2.079675	-2.079675	-2.079675	-2.079675	-2.079675
	TSDT (εz=0)	-2.079675	-2.079675	-2.079675	-2.079675	-2.079675
	Present (εz≠0)	**-2.286585**	**-2.286585**	**-2.286585**	**-2.286585**	**-2.286585**
1	Houri et al.[13] (εz≠0)	-2.277311	-2.482321	-2.639491	-2.383671	-2.653105
	Zenkour et al.[5] (εz≠0)	-2.277311	-2.482321	-2.639491	-2.383671	-2.653105
	Zenkour et al.[5] (εz=0)	-1.993885	-2.144369	-2.261939	-0.071622	-2.276155
	TSDT (εz=0)	-1.993921	-2.144422	-2.262000	-2.071668	-2.276209
	Present (εz≠0)	**-2.277050**	**-2.482052**	**-2.639221**	**-2.383405**	**-2.652839**
2	Houri et al.[13] (εz≠0)	-2.047272	-2.268798	-2.465763	-2.154066	-2.492766
	Zenkour et al.[5] (εz≠0)	-2.047272	-2.268798	-2.465763	-2.154066	-2.492766
	Zenkour et al.[5] (εz=0)	-1.824065	-1.982233	-2.127124	-1.899672	-2.152815
	TSDT (εz=0)	-1.824089	-1.982285	-2.127193	-1.899711	-2.152872
	Present (εz≠0)	**-2.047014**	**-2.268518**	**-2.465474**	**-2.153798**	**-2.492484**
3	Houri et al.[13] (εz≠0)	-1.963621	-2.173723	-2.384720	-2.058212	-2.421808
	Zenkour et al.[5] (εz≠0)	-1.963621	-2.173723	-2.384720	-2.058212	-2.421808
	Zenkour et al.[5] (εz=0)	-1.764689	-1.911970	-2.065398	-1.830216	-2.099241
	TSDT (εz=0)	-1.764705	-1.912017	-2.065467	-1.830246	-2.099296
	Present (εz≠0)	**-1.963372**	**-2.173445**	**-2.384425**	**-2.057951**	**-2.421522**
4	Houri et al.[13] (εz≠0)	-1.926265	-2.122027	-2.338550	-2.009198	-2.383070
	Zenkour et al.[5] (εz≠0)	-1.926265	-2.122027	-2.338550	-2.009198	-2.383070
	Zenkour et al.[5] (εz=0)	-1.738915	-1.874521	-2.030732	-1.795543	-2.070371
	TSDT (εz=0)	-1.738925	-1.874564	-2.030800	-1.795568	-2.070424
	Present (εz≠0)	**-1.926022**	**-2.121753**	**-2.338253**	**-2.008939**	**-2.382781**
5	Houri et al.[13] (εz≠0)	-1.907167	-2.090296	-2.309021	-1.980712	-2.359110
	Zenkour et al.[5] (εz≠0)	-1.907167	-2.090296	-2.309021	-1.980712	-2.359110
	Zenkour et al.[5] (εz=0)	-1.726003	-1.851867	-2.008794	-1.775738	-2.052671
	TSDT (εz=0)	-1.726010	-1.851906	-2.008861	-1.775759	-2.052722
	Present (εz≠0)	**-1.906922**	**-2.090025**	**-2.308724**	**-1.980463**	**-2.358822**

Table 5.

p	Theory	$\bar{\tau}_{xz}$				
		1-0-1	1-1-1	1-2-1	2-1-2	2-2-1
0	Houri et al.[13] (εz≠0)	0.762438	0.762438	0.762438	0.762438	0.762438
	Zenkour et al.[5] (εz≠0)	0.762438	0.762438	0.762438	0.762438	0.762438
	Zenkour et al.[5] (εz=0)	0.574063	0.574063	0.574063	0.574063	0.574063
	TSDT (εz=0)	0.466349	0.466349	0.466349	0.466349	0.466349
	Present (εz≠0)	**0.647283**	**0.647299**	**0.647304**	**0.647293**	**0.647299**
1	Houri et al.[13] (εz≠0)	0.916983	0.911165	0.922812	0.905127	0.914313
	Zenkour et al.[5] (εz≠0)	0.916983	0.911165	0.922812	0.905127	0.914313
	Zenkour et al.[5] (εz=0)	0.696774	0.694817	0.705269	0.689077	0.697901
	TSDT (εz=0)	0.564059	0.559957	0.566925	0.556662	0.562231
	Present (εz≠0)	**0.776577**	**0.771795**	**0.781716**	**0.766516**	**0.774339**
2	Houri et al.[13] (εz≠0)	0.919218	0.905787	0.930546	0.894489	0.916889
	Zenkour et al.[5] (εz≠0)	0.919218	0.905787	0.930546	0.894489	0.916889
	Zenkour et al.[5] (εz=0)	0.696044	0.689620	0.711266	0.679194	0.699571
	TSDT (εz=0)	0.565881	0.556769	0.571546	0.550567	0.564062
	Present (εz≠0)	**0.778004**	**0.766879**	**0.788118**	**0.756985**	**0.776258**
3	Houri et al.[13] (εz≠0)	0.923419	0.896673	0.930393	0.883314	0.914156
	Zenkour et al.[5] (εz≠0)	0.923419	0.896673	0.930393	0.883314	0.914156
	Zenkour et al.[5] (εz=0)	0.697635	0.681516	0.710627	0.669256	0.696850
	TSDT (εz=0)	0.568711	0.551237	0.571319	0.544027	0.562514
	Present (εz≠0)	**0.781379**	**0.758865**	**0.787806**	**0.747194**	**0.773758**
4	Houri et al.[13] (εz≠0)	0.931204	0.888770	0.928612	0.875373	0.911369
	Zenkour et al.[5] (εz≠0)	0.931204	0.888770	0.928612	0.875373	0.911369
	Zenkour et al.[5] (εz=0)	0.702617	0.674664	0.708782	0.662291	0.694226
	TSDT (εz=0)	0.573625	0.546463	0.570117	0.539446	0.560893
	Present (εz≠0)	**0.787952**	**0.752051**	**0.786182**	**0.740374**	**0.771341**
5	Houri et al.[13] (εz≠0)	0.940770	0.882525	0.926543	0.870190	0.909225
	Zenkour et al.[5] (εz≠0)	0.940770	0.882525	0.926543	0.870190	0.909225
	Zenkour et al.[5] (εz=0)	0.709315	0.669326	0.706821	0.657748	0.692220
	TSDT (εz=0)	0.579530	0.542724	0.568771	0.536526	0.559642
	Present (εz≠0)	**0.796105**	**0.746661**	**0.784368**	**0.735758**	**0.769403**

Table 6.

p	Theory	$\bar{\tau}_{xz}$				
		1-0-1	1-1-1	1-2-1	2-1-2	2-2-1
0	**Present**[a] (εz≠0)	0.843140	0.843148	0.843153	0.843141	0.843147
	Present[b] (εz≠0)	0.779757	0.779754	0.779757	0.779753	0.779755
	Present[c] (εz≠0)	**0.903551**	**0.903544**	**0.903551**	**0.903553**	**0.903553**
1	**Present**[a] (εz≠0)	1.008621	1.001380	1.013835	0.994964	1.004650
	Present[b] (εz≠0)	0.926195	0.917266	0.927741	0.912356	0.920192
	Present[c] (εz≠0)	**1.088556**	**1.083387**	**1.097958**	**1.075332**	**1.087015**
2	**Present**[a] (εz≠0)	1.011299	0.995136	1.021869	0.983042	1.007090
	Present[b] (εz≠0)	0.930521	0.911855	0.934510	0.902449	0.922331
	Present[c] (εz≠0)	**1.089278**	**1.076289**	**1.107360**	**1.061264**	**1.089786**
3	**Present**[a] (εz≠0)	1.016334	0.985017	1.021510	0.970784	1.004005
	Present[b] (εz≠0)	0.936610	0.903197	0.934292	0.892227	0.919872
	Present[c] (εz≠0)	**1.093012**	**1.064629**	**1.106852**	**1.046833**	**1.086030**
4	**Present**[a] (εz≠0)	1.025315	0.976379	1.019474	0.962232	1.000997
	Present[b] (εz≠0)	0.945861	0.895768	0.932590	0.885136	0.917448
	Present[c] (εz≠0)	**1.101542**	**1.054721**	**1.104461**	**1.036717**	**1.082395**
5	**Present**[a] (εz≠0)	1.036215	0.969546	1.017179	0.956512	0.998612
	Present[b] (εz≠0)	0.956571	0.889871	0.930629	0.880430	0.915513
	Present[c] (εz≠0)	**1.112492**	**1.046906**	**1.101814**	**1.029908**	**1.079525**

[a] $\Psi(z) = (h/\pi)\sin(\pi z/h)$

[b] $\Psi(z) = z\left(1-(4/3)(z/h)^2\right)$

[c] $\Psi(z) = ze^{-2(z/h)^2}$

Figures

Figure 1.

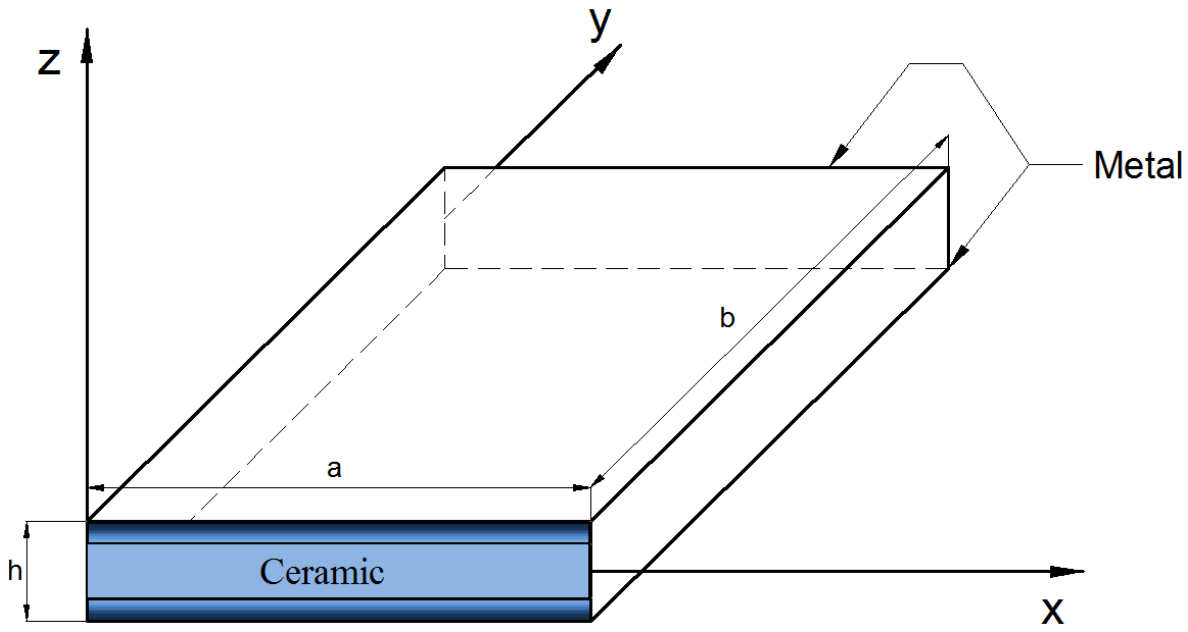

Figure 2.

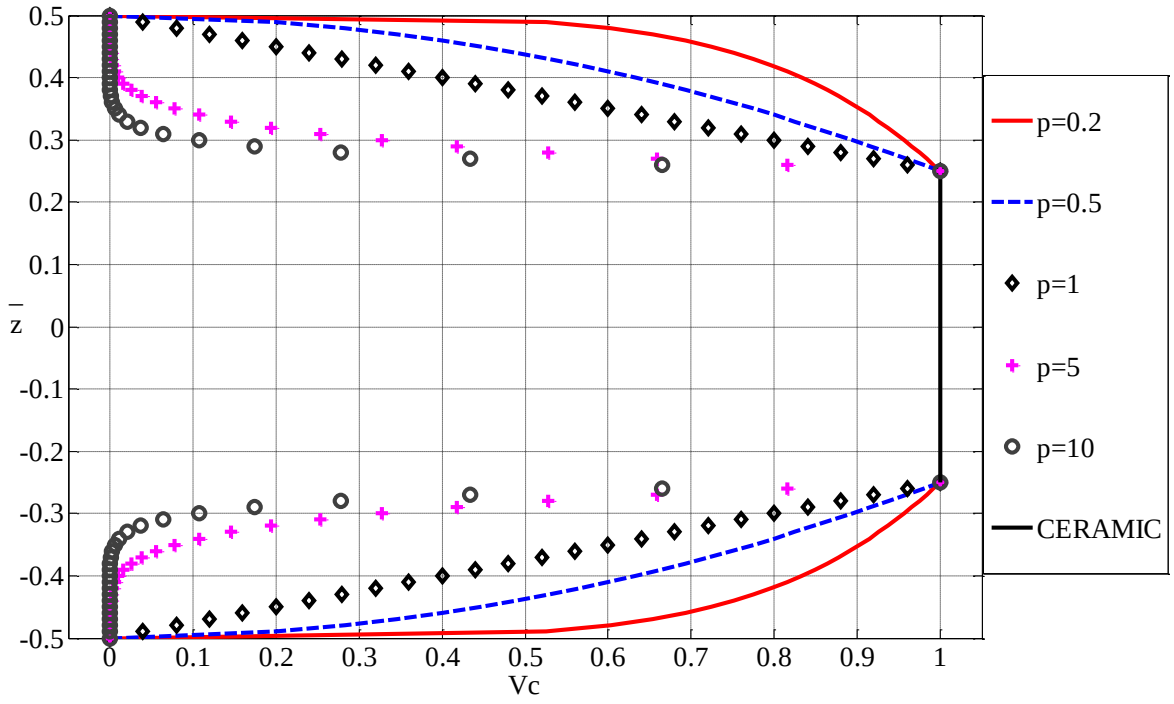
0.5
0.4
0.3
0.2
0.1
0
-0.1
-0.2
-0.3
-0.4
-0.5
z
0
0.1
0.2
0.3
0.4
0.5
0.6
0.7
0.8
0.9
1
Vc
p=0.2
p=0.5
p=1
p=5
p=10
CERAMIC

Figure 3.

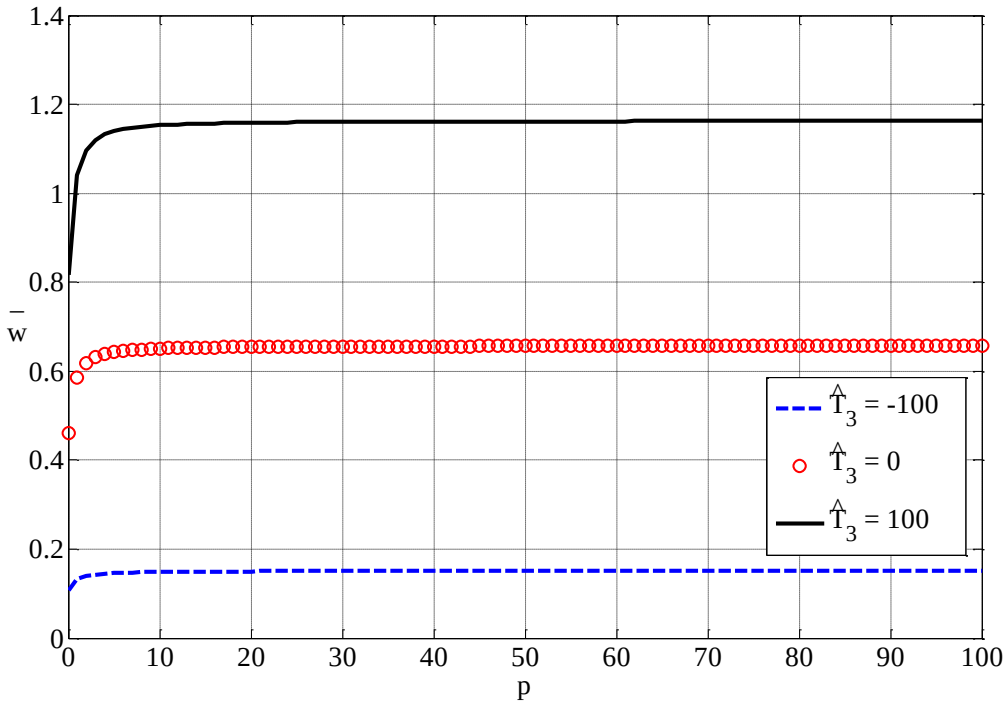
1.4
1.2
1
0.8
0.6
0.4
0.2
0
w̄
0
10
20
30
40
50
60
70
80
90
100
p
T̂3 = -100
T̂3 = 0
T̂3 = 100

Figure 4.

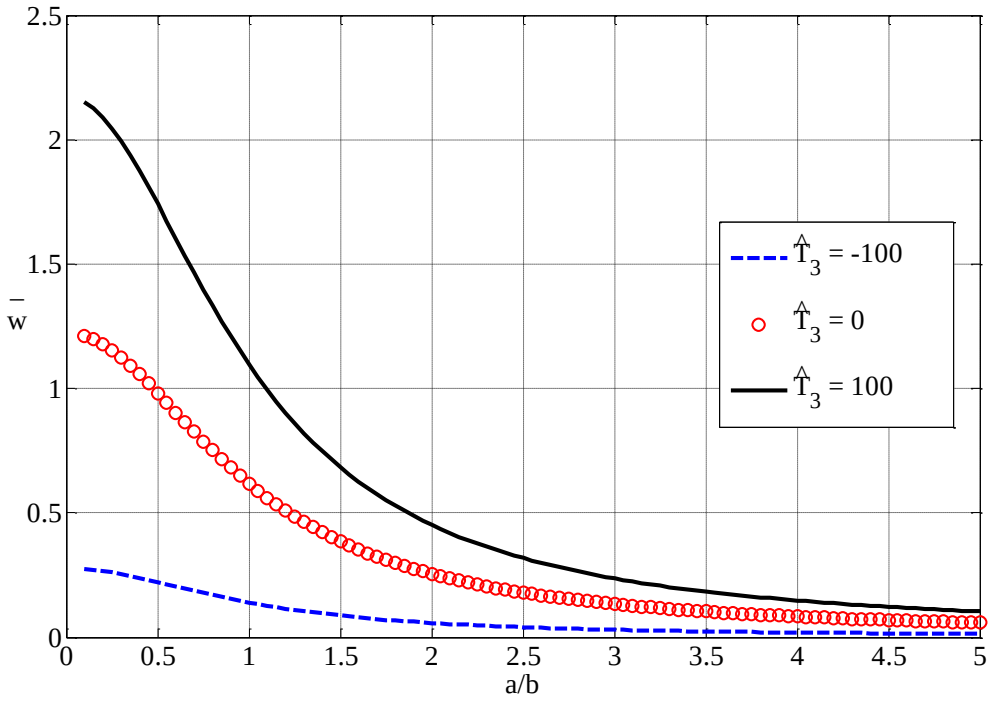
2.5
2
1.5
1
0.5
0
$\bar{w}$
0
0.5
1
1.5
2
2.5
3
3.5
4
4.5
5
a/b
$\hat{T}_3$ = -100
$\hat{T}_3$ = 0
$\hat{T}_3$ = 100

Figure 5.

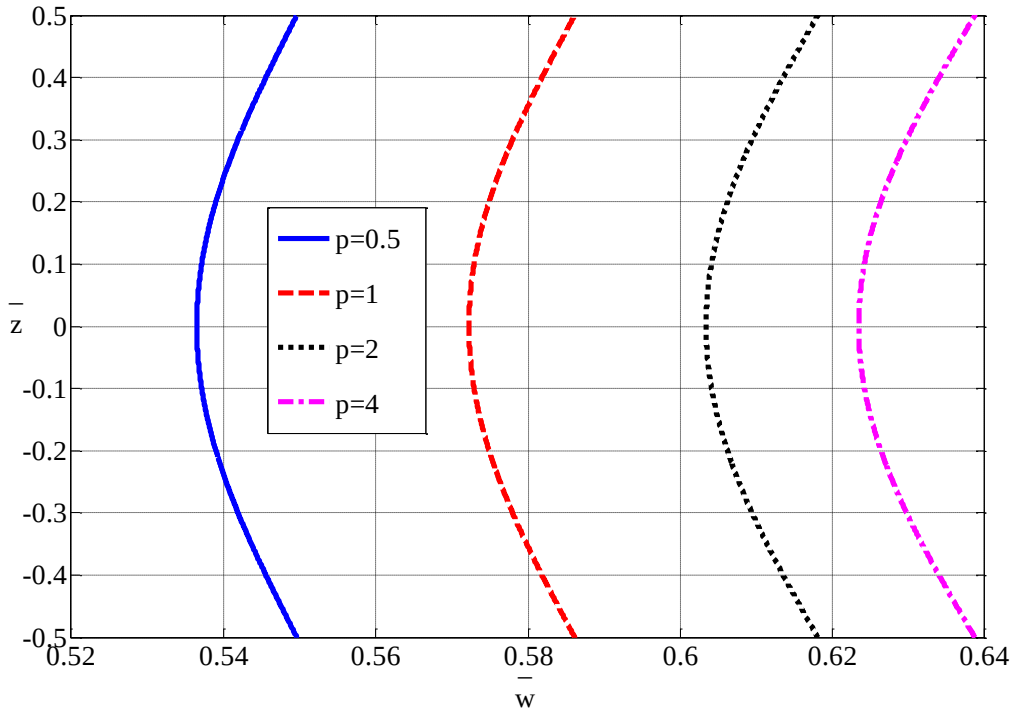
0.5
0.4
0.3
0.2
0.1
0
-0.1
-0.2
-0.3
-0.4
-0.5
z̄
0.52
0.54
0.56
0.58
0.6
0.62
0.64
w̄
p=0.5
p=1
p=2
p=4

Figure 6.

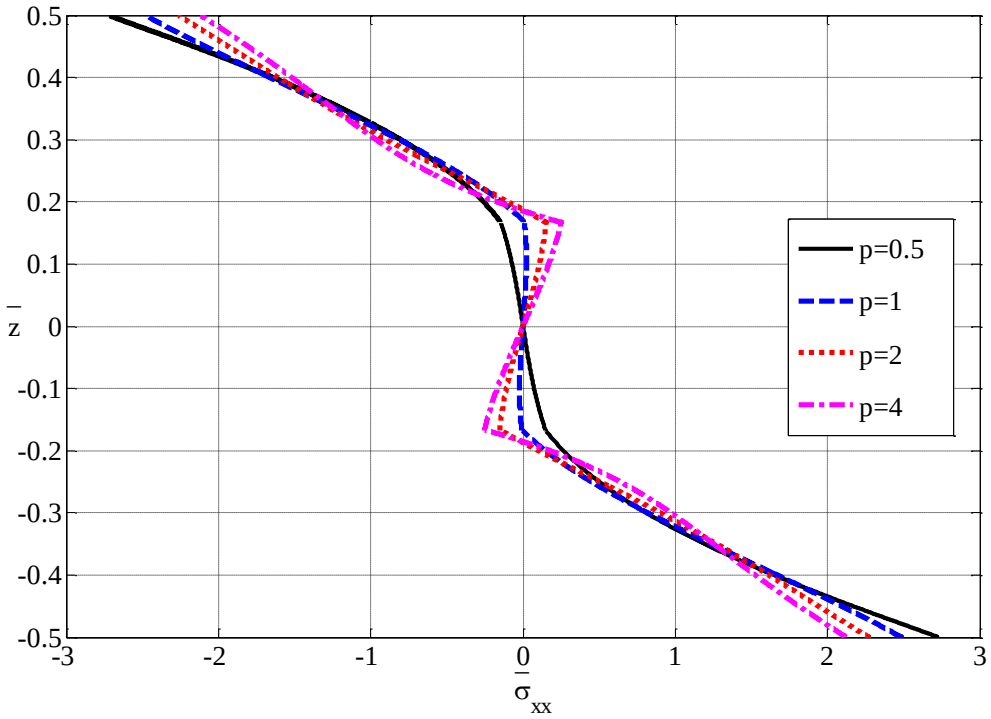

Figure 7.

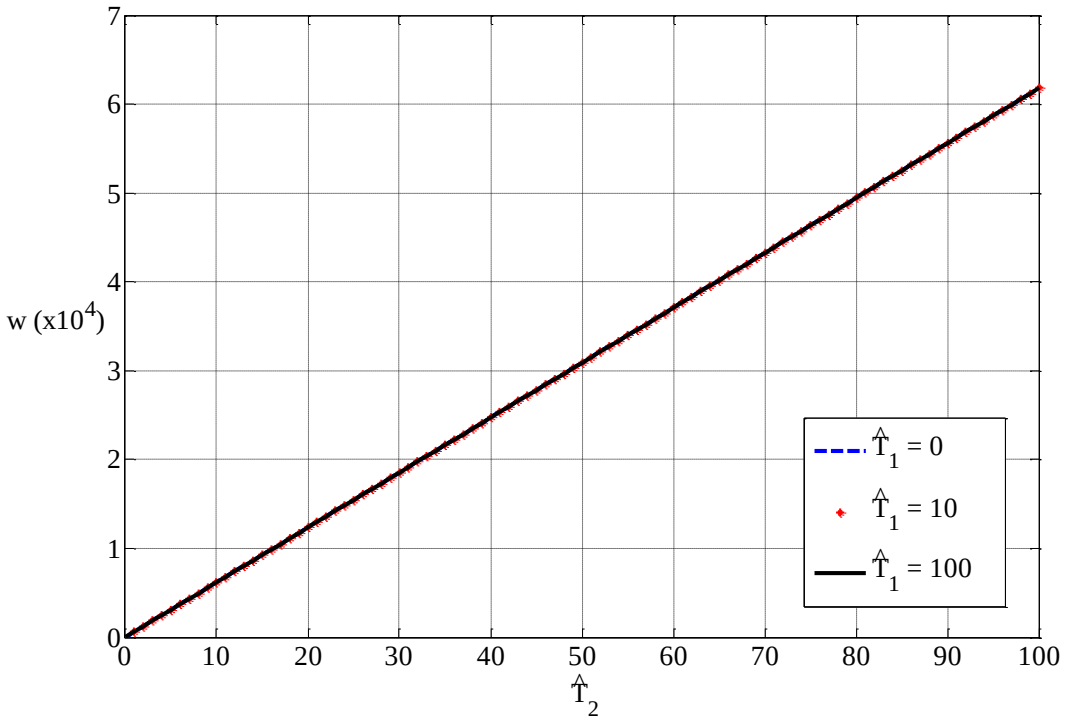

Figure 8.

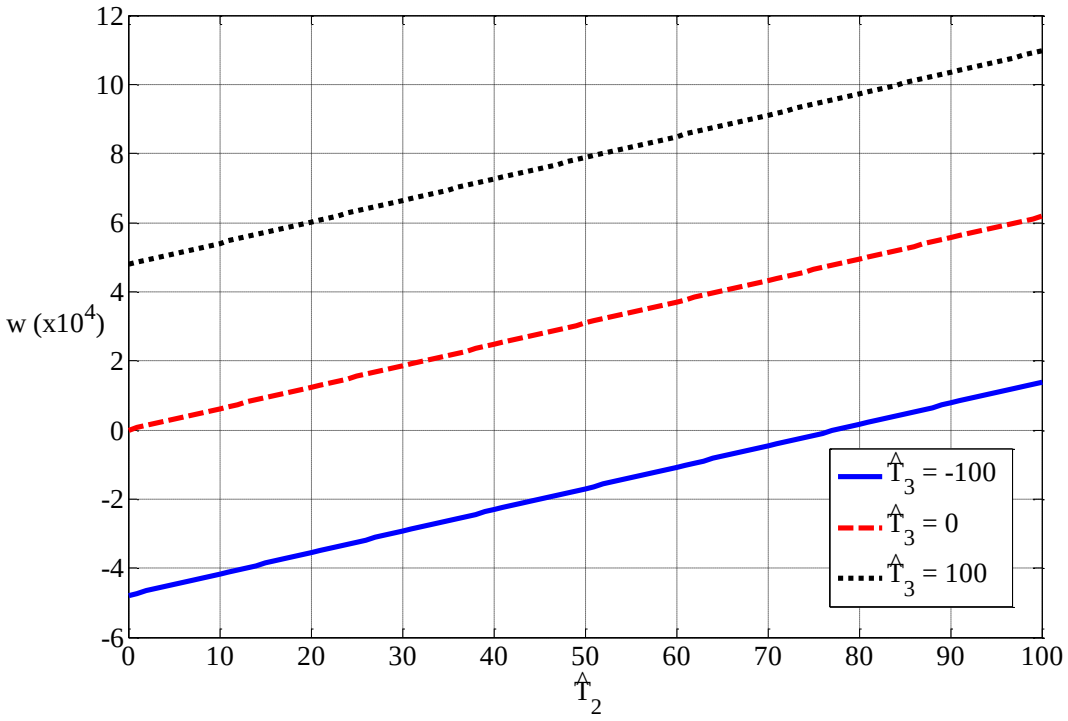
w (x10^4)
12
10
8
6
4
2
0
-2
-4
-6
0
10
20
30
40
50
60
70
80
90
100
T̂2
T̂3 = -100
T̂3 = 0
T̂3 = 100

Figure 9.

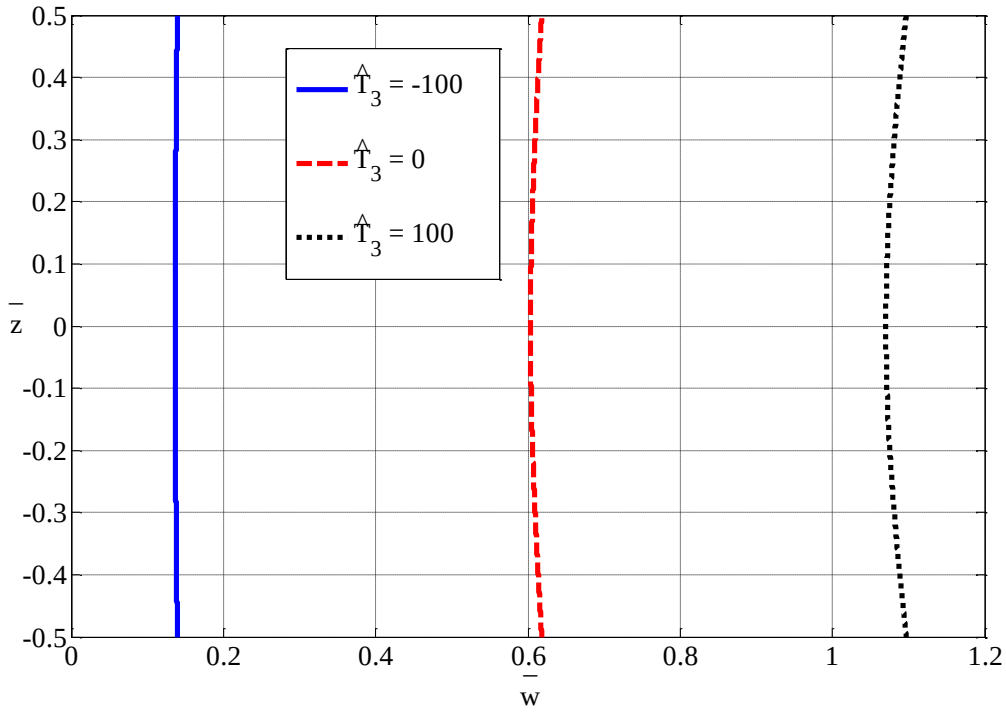

Figure 10.

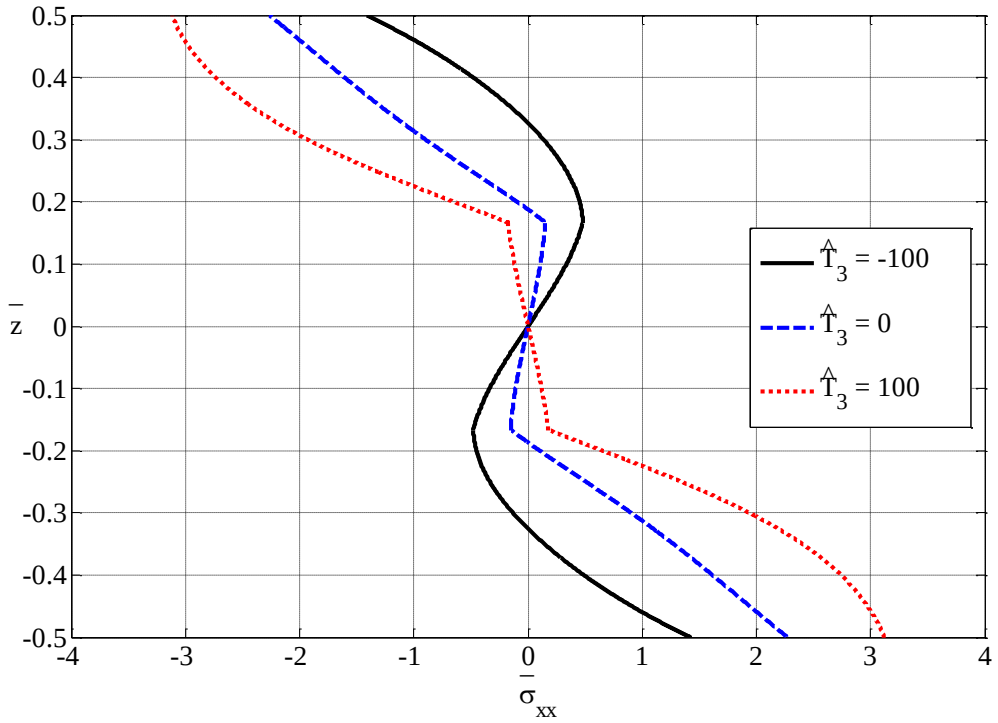

Figure 11.

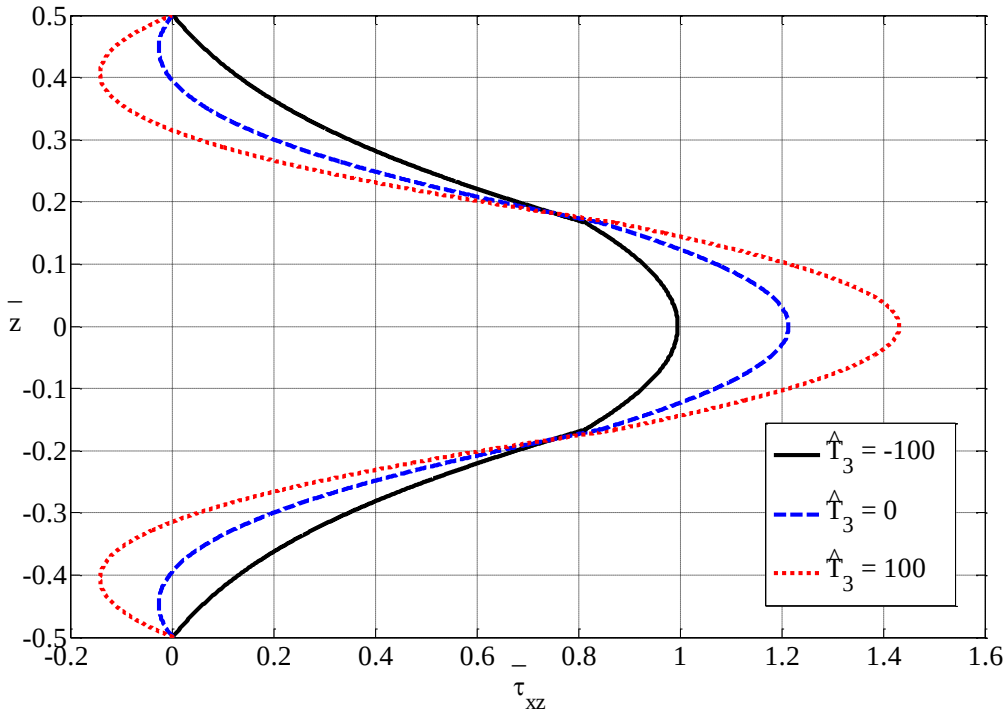
0.5
0.4
0.3
0.2
0.1
0
-0.1
-0.2
-0.3
-0.4
-0.5
z
-0.2
0
0.2
0.4
0.6
0.8
1
1.2
1.4
1.6
τxz
T3 = -100
T3 = 0
T3 = 100